



Design, evaluation and future projections of the NARClIM2.0 CORDEX-CMIP6 Australasia regional climate ensemble

Giovanni Di Virgilio^{1,2}, Jason P. Evans^{2,3}, Fei Ji^{1,3}, Eugene Tam¹, Jatin Kala⁴, Julia Andrys⁴, Christopher Thomas², Dipayan Choudhury¹, Carlos Rocha¹, Stephen White¹, Yue Li¹, Moutassem El Rafei¹, Rishav Goyal¹, Matthew L. Riley¹ and Jyothi Lingala⁴

¹Climate & Atmospheric Science, NSW Department of Climate Change, Energy, the Environment and Water, Sydney, Australia

²Climate Change Research Centre, University of New South Wales, Sydney, Australia

³Australian Research Council Centre of Excellence for Climate Extremes, University of New South Wales, Sydney, Australia

⁴Environmental and Conservation Sciences, and Centre for Climate Impacted Terrestrial Ecosystems, Harry Butler Institute, Murdoch University, Murdoch, WA 6150, Australia

Correspondence to: Giovanni Di Virgilio (giovanni.divirgilio@environment.nsw.gov.au;
giovanni@unsw.edu.au)

1 **Abstract.** NARClIM2.0 comprises two Weather Research and Forecasting (WRF) regional climate
2 models (RCMs) downscaling five CMIP6 global climate models contributing to the Coordinated
3 Regional Downscaling Experiment over Australasia at 20 km resolution, and south-east Australia at 4
4 km convection-permitting resolution. We first describe NARClIM2.0's design, including selecting
5 two, definitive RCMs via testing seventy-eight RCMs using different parameterisations for planetary
6 boundary layer, microphysics, cumulus, radiation, and land surface model (LSM). We then assess
7 NARClIM2.0's skill in simulating the historical climate versus CMIP3-forced NARClIM1.0 and
8 CMIP5-forced NARClIM1.5 RCMs and compare differences in future climate projections. RCMs
9 using the new Noah-MP LSM in WRF with default settings confer substantial improvements in
10 simulating temperature variables versus RCMs using Noah-Unified. Noah-MP confers smaller
11 improvements in simulating precipitation, except for large improvements over Australia's southeast
12 coast. Activating Noah-MP's dynamic vegetation cover and/or runoff options primarily improve
13 simulation of minimum temperature. NARClIM2.0 confers large reductions in maximum temperature
14 bias versus NARClIM1.0 and 1.5 (1.x), with small absolute biases of ~0.5K over many regions versus
15 over ~2K for NARClIM1.x. NARClIM2.0 reduces wet biases versus NARClIM1.x by as much as
16 50%, but retains dry biases over Australia's north. NARClIM2.0 is biased warmer for minimum
17 temperature versus NARClIM1.5 which is partly inherited from stronger warm biases in CMIP6



18 versus CMIP5 GCMs. Under shared socioeconomic pathway (SSP)3-7.0, NARcliM2.0 projects ~3K
19 warming by 2060-79 over inland regions versus ~2.5K over coastal regions. NARcliM2.0-SSP3-7.0
20 projects dry futures over most of Australia, except for wet futures over Australia's north and parts of
21 western Australia which are largest in summer. NARcliM2.0-SSP1-2.6 projects dry changes over
22 Australia with only few exceptions. NARcliM2.0 is a valuable resource for assessing climate change
23 impacts on societies and natural systems and informing resilience planning by reducing model biases
24 versus earlier NARcliM generations and providing more up-to-date future climate projections
25 utilising CMIP6.

Keywords:

26 Climate change; climate impact adaptation; dynamical downscaling; CORDEX-CMIP6; model
27 design; model evaluation



28 **1. Introduction**

29 Climate projections are foundational to informing climate change mitigation and adaptation planning
30 at various spatial scales (IPCC, 2021). Regional climate models (RCMs) dynamically downscale
31 global climate models (GCMs) at ~100-200 km resolution to simulate higher resolution climate
32 projections that better resolve local-scale influences on regional climate, such as mountain ranges,
33 land-use variation, land-sea contrasts, and convective processes (Torma et al., 2015; Giorgi, 2019). As
34 such, whilst GCMs are the best tools for investigating climate at global scales, RCMs provide
35 improved guidance for climate policy at regional scale, which is the scale at which climate change
36 impacts are experienced (Hsiang et al., 2017).

37 The NARClIM programme (New South Wales and Australian Regional Climate Modelling) is
38 now in its third generation. Like its predecessors, NARClIM version 2.0 ('NARClIM2.0'), aims to
39 produce robust, detailed regional climate projections at spatial scales relevant for use in local-scale
40 climate change analysis. A key feature of all NARClIM generations is to simulate the climate over the
41 Coordinated Regional Downscaling Experiment (CORDEX)-Australasia domain, and a higher
42 resolution inner domain over southeast Australia via one-way nesting (Figure 1). With one-way
43 nesting the inner domain obtains its initial and lateral boundary conditions from the simulation over
44 CORDEX-Australasia. NARClIM1.0 simulated the climate of Australasia for three periods (1990-
45 2009, 2020-2039, 2060-2079) at 50 km resolution and southeast Australia at 10 km using three
46 configurations of the weather research and forecasting (WRF) RCM (Skamarock et al., 2008) to
47 downscale GCMs from Coupled Model Intercomparison Project phase three (CMIP3) under the SRES
48 A2 greenhouse gas (GHG) scenario (Evans et al., 2014). NARClIM1.5 used CMIP5 GCMs under
49 representative concentration pathways (RCP) 4.5 and 8.5 to simulate continuously for 1950-2100 on
50 the same grids as NARClIM1.0 using two of its RCMs (Nishant et al., 2021).

51 NARClIM2.0 aims to improve performance in simulating the Australian climate relative to
52 previous NARClIM generations with the goal of better informing community resilience to climate
53 change (New South Wales Government, 2022, 2023). All NARClIM projects include a bottom-up
54 design ethos involving multi-sectoral end-user engagement in specifying model requirements to
55 ensure model performance and outputs meet end-user needs. Key requirements from the NARClIM2.0
56 user-consultation include providing increased detail in climate simulations via higher resolution, and
57 improving the simulation of precipitation and temperature as these are fundamental inputs to climate
58 impact studies. Whilst NARClIM1.0 and 1.5 (1.x) confer the expected level of performance in
59 simulating the Australian climate (Di Virgilio et al., 2019; Evans et al., 2020b), recent technological
60 and scientific advancements mean that aspects of their performance might now be improved.
61 NARClIM1.x RCMs show widespread cold biases in maximum temperature exceeding -5K for some
62 RCMs. Conversely, minimum temperature is simulated more accurately with biases in the range of



63 $\pm 1.5\text{K}$. NARClIM1.x RCMs overestimate precipitation, particularly over Australia's socio-
64 economically important eastern seaboard (Di Virgilio et al., 2019).

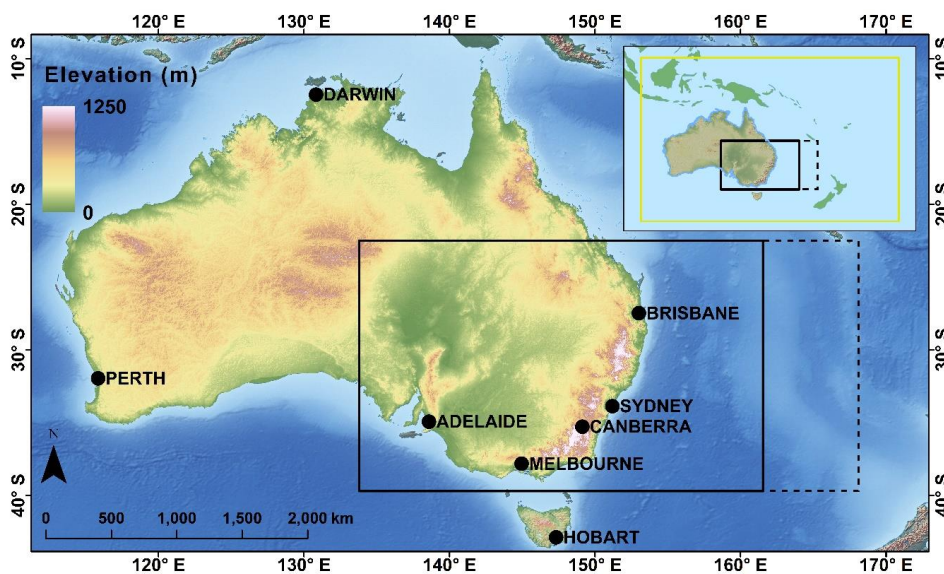
65 As they are expensive to run from both computational and data storage perspectives, dynamical
66 downscaling projects like NARClIM2.0 use a subset of available GCMs as driving data, necessitating
67 careful model selection. Similarly, a large combination of different physical parametrisations
68 available for the WRF RCM enables many structurally different RCMs to be potentially used to
69 downscale GCMs. A key component of NARClIM2.0's design is testing the viability of alternative
70 RCM parameterisations via a three-phase approach, with each phase building on the preceding phase
71 to identify the RCM parameterisations that perform well during testing to meet NARClIM2.0's aim of
72 improving the simulation of Australia's climate. GCM and RCM statistical independence are also
73 sought to avoid creating a biased sample of climate change. Hence, the aims of this paper are to:

74 1) describe how and why NARClIM2.0 differs from its predecessors in terms of its design and
75 production processes, explaining the model test and evaluation approaches underlying its design
76 decisions. A key focus is on the design and testing of seventy-eight different WRF RCMs and their
77 evaluation to identify a subset of RCMs for use in NARClIM2.0;

78 2) characterise the performance improvements of CMIP6-NARClIM2.0 RCMs in simulating the
79 Australian climate relative to previous NARClIM generations by evaluating their skill in simulating
80 mean maximum and minimum temperature and precipitation versus observations;

81 and 3) summarise the climate projections produced by CMIP6-NARClIM2.0 and how these
82 differ from previous CMIP3-5-NARClIM generations.

83 The following section summarises the basic design features of each NARClIM generation;
84 section 3. describes NARClIM2.0's design process with a focus on its RCM physics testing, as well as
85 a brief overview of its production process; section 4. describes evaluation methods and metrics;
86 section 5. summarises the RCM physics test results; section 6. evaluates the performance of all
87 NARClIM models in simulating the recent Australian climate; section 7. provides an overview of their
88 future projections; and section 8. discusses key results and summarises this paper.



89

90 **Figure 1.** Model domains for NARClIM regional climate simulations. The southeast inner domain for
91 NARClIM2.0 is delineated with a solid black rectangle; the corresponding inner domain for NARClIM1.0 and
92 1.5 is delineated with a dashed black line. The elevated terrain of the Australian Alps which form part of the
93 Great Dividing Range is in eastern Australia. Inset shows the CORDEX-Australasia outer domain.

94 **2. Three generations of NARClIM: model overviews**

95 The design of NARClIM1.0 is described in Evans et al. (2014); NARClIM1.5 used the same design
96 approach but used CMIP5 rather than CMIP3 GCMs. All generations of NARClIM use different
97 versions of the WRF model (Skamarock et al., 2008) to perform dynamical downscaling of GCMs
98 since the WRF model goes through regular updates. The southeast Australian inner domain captures
99 five of Australia's eight capital cities (Figure 1) and over 75% of the Australian population
100 (Australian Bureau Statistics, 2024). Additionally, the inner domain captures coastal regions that are
101 characterised by topographic complexity and land-use class variation. Regions east of the Great
102 Dividing Range mountains in southeast Australia (Figure 1) show different responses to oceanic
103 climate modes compared to inland semi-arid regions (Murphy and Timbal, 2008) and are impacted by
104 events such as rapidly developing storms, including east coast lows (Pepler and Dowdy, 2021). Such
105 atmospheric processes are not adequately resolved by GCMs due to coarse resolutions (Di Virgilio et
106 al., 2022; Grose et al., 2020).

107 NARClIM2.0 encompasses several design advancements over its predecessors (Table 1).
108 NARClIM2.0 RCMs have a 20 km resolution CORDEX-Australasia domain (versus 50 km) and 4 km
109 (versus 10 km) domain over southeast Australia and use 45 (versus 30) vertical levels. The aim of



110 increasing the resolution of this inner domain from 10 km to 4 km is to render these simulations
111 convection-permitting (Kendon et al., 2021; Lucas-Picher et al., 2021). Hence, whilst the 20 km-
112 resolution outer domain uses cumulus parametrisation, simulations over the 4 km domain do not use
113 cumulus parametrisation. NARcliM2.0 also includes a new collaboration with the Western Australian
114 government, with separate 4 km simulations being performed over south-west and north-west Western
115 Australia (not shown in Figure 1) as part of the Western Australian climate science initiative (DWER,
116 2023). Boundary conditions derived from the 20 km NARcliM2.0 CORDEX Australasia domain are
117 used to drive these simulations. Additional major differences in model setup for NARcliM2.0
118 include:

- 119 ▪ NARcliM1.0 RCMs use different parameterisations for planetary boundary layer (PBL)
120 physics, surface physics, cumulus physics, land surface model (LSM), and radiation (Evans et
121 al., 2014). These RCM parameterisations were also used for NARcliM1.5. Owing to the pro-
122 ject aims stated above, RCM parameterisations for NARcliM2.0 differ to those of NAR-
123 cliM1.x (see sect. 3).
- 124 ▪ NARcliM2.0 increases the number of driving GCMs to 5 and simulates for a wider range of
125 plausible future climates via three shared socioeconomic pathways (SSP). SSP1-2.6 is select-
126 ed as a low GHG scenario envisaging a future climate with CO₂ emissions cut to net zero by
127 around 2075 and warming held to below 2°C by 2100; SSP2-4.5 estimates projected warming
128 under a ‘middle of the road’ scenario where temperatures increase to ~2.7°C by 2100; and
129 SSP3-7.0 is a high GHG scenario which assumes warming of ~4°C by 2100 (IPCC, 2021).
- 130 ▪ Urban physics is activated in NARcliM2.0 (WRF setting: sf_urban_physics=1) to represent
131 surface energy balance in urban areas via a single layer urban canopy model (Kusaka and
132 Kimura, 2004).
- 133 ▪ Input of different aerosol species is activated for the RCM radiation scheme using the Tegen
134 et al. (1997) climatology available in WRF (aer_opt=1). This aerosol forcing is the same for
135 all GCMs, and not model-specific.
- 136 ▪ The eastern boundary of the NARcliM2.0 inner domain is located further westward relative
137 to that of NARcliM1.x (Figure 1).



138 **Table 1.** High-level design features of three generations of NARClIM regional climate models

	Model Generation		
	NARClIM1.0	NARClIM1.5	NARClIM2.0
Release date	2014	2020	2023-2024
Years simulated	1990-2009, 2020-2039, 2060-2079	1950-2100	1950-2100
Grid resolutions: CORDEX-Australasia; NARClIM inner domains	50 km; 10 km	50 km; 10 km	20 km; 4 km
Vertical levels	30	30	45
Global Climate Models	4 CMIP3 GCMs	3 CMIP5 GCMs	5 CMIP6 GCMs
Regional Climate Models	3 RCM configurations (WRF3.3)	2 RCM configurations (WRF3.6.0.5)	2 RCM configurations (WRF4.1.2)
Future emission scenarios	SRES A2	RCP4.5, RCP8.5	SSP1-2.6, SSP2-4.5, SSP3-7.0
Reanalysis-driven (CORDEX Evaluation)	NCEP: 1950-2009	ERA-Interim: 1979-2013	ERA5: 1979-2020

139 **3. NARClIM2.0 design and production process overview**

140 The NARClIM2.0 design and production processes are summarised below in reference to Figure 2.
 141 The design process is an adaptation of that introduced in Evans et al. (2014). Two companion
 142 manuscripts describe elements shown in Figure 2, and which are therefore only summarised briefly in
 143 this manuscript. Di Virgilio et al. (2022) describes the CMIP6 GCM selection process summarised in
 144 Box 2, and Di Virgilio et al. (in review) describes the ERA5 evaluation undertaken in Boxes 5 and 6.

145 **I. Design Phase:**

- 146 i) **Box 1:** model design requirements are identified via consultation between NARClIM2.0
 147 modelling groups and multi-sectoral end-users, as well as adherence to CORDEX-CMIP6
 148 design requirements (WCRP, 2020).



- 149 ii) **Box 2:** NARClIM1.x selected driving CMIP3-5 GCMs (respectively) via literature review
150 of existing GCM evaluations. During NARClIM2.0 design, there were no pre-existing
151 comprehensive evaluations of individual CMIP6 GCMs for the Australian region, includ-
152 ing assessments of climate change signals and GCM statistical independence. Hence, an
153 evaluation and selection of CMIP6 GCMs was conducted (see Di Virgilio et al. 2022).
154 This evaluation selected five GCMs to force two NARClIM2.0 RCMs (see sect 3.2 and
155 3.4). The relative contribution to uncertainty/variation in climate projections can be larger
156 for GCMs than for RCMs (e.g. Lee et al., 2023).
- 157 iii) **Box 3:** a new WRF RCM multi-physics test ensemble is created for NARClIM2.0: RCM
158 physics testing is conducted via a three-phase approach, with each phase building on the
159 findings of the preceding phase to identify the RCM parameterisations that perform well
160 during testing with the aim of improving the simulation of the Australian climate. In this
161 way, RCMs are parameterised with different physics settings via each test phase, system-
162 atically removing poor performing options while facilitating the fine tuning and im-
163 provement of the parameterisations that perform well during testing to build a total en-
164 semble size of seventy-eight structurally different test RCMs. The performances of the
165 different test RCM configurations are evaluated, ultimately selecting a subset of seven
166 RCMs for subsequent downscaling of ERA5 reanalysis and comprising the CORDEX
167 evaluation experiment.
- 168 iv) **Boxes 4-6:** These seven RCMs are used to downscale ERA5 reanalysis over the 20 km
169 and 4 km domains for 1979-2020. Evaluating these ERA5-forced simulations informs se-
170 lection of two ‘production’ RCMs for CMIP6-forced downscaling (see sect. 3.4 and Di
171 Virgilio et al. in review).

172 II. Production Phase:

- 173 i) **Boxes 7-8:** CMIP6 GCM data are pre-processed to create initial and boundary conditions
174 to drive simulations for the historical (1950-2014) and SSP experiments (2015-2100). A
175 code repository used for this GCM preprocessing is available at
176 [https://bitbucket.org/oehtcas/narclim2-](https://bitbucket.org/oehtcas/narclim2-0_design_and_evaluation_2024_support_materials/src/main/)
177 [0 design and evaluation 2024 support materials/src/main/](https://bitbucket.org/oehtcas/narclim2-0_design_and_evaluation_2024_support_materials/src/main/) within the
178 WRF/repo_snapshots subdirectory. Quality assurance/quality control (QA/QC) is per-
179 formed on these data before initiating the simulations (e.g. variables are checked to con-
180 firm data do not contain significant outliers across ensemble members).
- 181 ii) **Boxes 9-11:** the 151-year CMIP6-forced NARClIM2.0 RCM simulations are run using
182 National Computing Infrastructure at Canberra, Australia (NCI, <https://nci.org.au/>). File
183 integrity verification and QA/QC are performed on each year of raw WRF output
184 throughout the simulation lifecycle and prior to post-processing to CORDEX-compliant



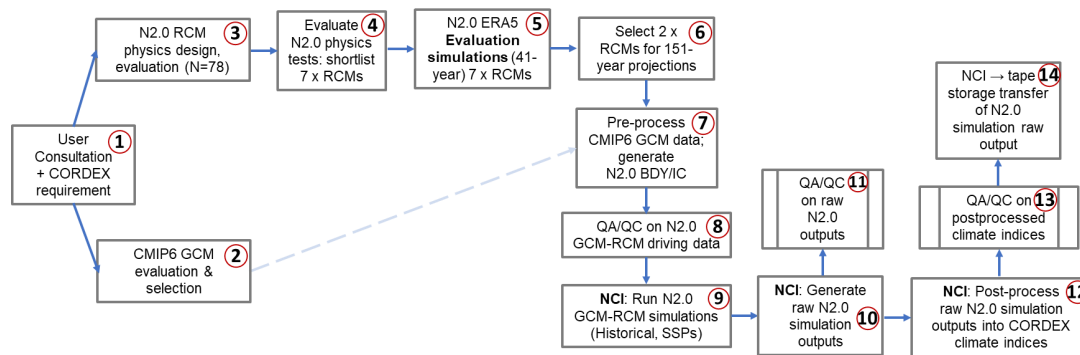
185 format climate variables. QA/QC tests include calculating the minimum, maximum, mean
186 and standard deviation for key variables over consecutive periods of six days. Variables
187 are categorised as either normally distributed or otherwise. Normally distributed variables
188 (e.g. surface temperature) are deemed potentially erroneous if their minima/maxima are
189 greater than five standard deviations away from the global mean of the relevant statistic
190 of the rolling six-day period. Non-normally distributed variables (e.g. snow depth and
191 precipitation) are checked for global minima and maxima only.

192 iii) **Boxes 12-13:** after each year of simulation raw output is generated, their post-processing
193 is initiated to produce CORDEX CORE, Tier 1 and Tier 2 variables (WCRP, 2022). A
194 statistical QA/QC process is automatically applied to each year of post-processed
195 CORDEX CORE variables as they are generated throughout the simulations. QA/QC
196 tests include:

- 197 ▪ Check for presence of missing values.
- 198 ▪ Check that all values are within realistic ranges for minima and maxima.
- 199 ▪ Check minima and maxima are not equal at any timestep with exceptions (e.g.
200 snow depth which can be zero everywhere in the outer domain).
- 201 ▪ Check that changes over time are within realistic ranges (i.e. assess temporal gra-
202 dients).
- 203 ▪ Check that changes between neighbouring data points are within realistic ranges
204 (i.e. assess spatial gradients).
- 205 ▪ Check the number of grid cells with NaN (non-numerical) values do not exceed
206 the threshold set for the variable.

207 Reasonable ranges for variables are determined using a series of threshold values that are
208 based on historical records and/or empirical analysis. QA/QC computer scripts generate
209 'exceedance files' which output every data point that surpasses the threshold values, and
210 these exceedance files are then manually reviewed to determine whether an issue is a true
211 or false positive, etc.

212 iv) **Box 14:** Once each year of WRF raw files are post-processed, raw files are transferred to
213 a tape facility for long-term storage.



214

215 **Figure 2.** Simplified overview of NARClIM2.0 (N2.0) design and production processes. ERA5 = ECMWF
216 Reanalysis v5 data; BDY = boundary conditions; IC = Initial conditions; QA/QC = Quality Assurance / Quality
217 Control; NCI = National Computing Infrastructure (high performance computer used for N2.0 production
218 simulations).

219 These model design and production stages are now described in more detail:

220 3.1 Model evaluation and selection

221 Practical constraints such as available compute and data storage resources enforce an upper limit on
222 GCM-RCM ensemble size. Thus, NARClIM2.0 uses a subset of available CMIP6 GCMs and WRF
223 RCM configurations, necessitating careful GCM and RCM selection to create a subset of GCM-
224 RCMs that provide robust climate simulations whilst also adequately sampling model uncertainty. In
225 selecting a subset of GCMs and RCMs for dynamical downscaling, it is desirable to reject models that
226 perform consistently poorly relative to their peers in simulating the current climate, as this provides
227 lower confidence in the projected change (Evans et al., 2020b; Di Virgilio et al., 2022; Grose et al.,
228 2023). Furthermore, the modelled climate space sampled is reduced when selecting a subset of GCMs,
229 which can create a biased view of the climate, as well as the plausible change in climate. Care must
230 therefore be taken to ensure that the subset of models used for downscaling are representative of the
231 full range of possible climates, and that model errors are uncorrelated, i.e., that models are statistically
232 independent. The steps taken to evaluate and select GCMs and RCMs for NARClIM2.0 are described
233 next.

234 3.2 CMIP6 GCM evaluation

235 A three-phase process was used to evaluate individual CMIP6 GCMs (for further details see Di
236 Virgilio et al. 2022):



237 **3.2.1 CMIP6 GCM Performance**

238 The performances of individual CMIP6 GCMs in simulating the Australian climate were assessed
239 with respect to climate means, extremes, climate modes, and daily climate variable distributions. A set
240 of GCMs that performed consistently poorly across the variables and statistics considered were
241 identified. These models, as well as those with insufficient data to enable dynamical downscaling
242 using the WRF RCM, were excluded from further evaluation leaving 27 GCMs for subsequent
243 assessment.

244 **3.2.2 CMIP6 GCM Independence**

245 The retained 27 GCMs were subjected to the Bishop and Abramowitz (2013) and Herger et al. (2018)
246 independence analyses (see sect. 4.4). The GCMs were then ranked according to their relative level of
247 statistical independence.

248 **3.2.3 Sampling CMIP6 GCM Climate Change Spread**

249 For climate change risk assessments, climate projections should reflect as much of the range of
250 plausible future climate changes as possible (Whetton and Hennessy, 2010). The subset of CMIP6
251 GCMs selected for NARClIM2.0 spanned a wide range of future changes in annual mean temperature
252 and precipitation. Climate change signals were calculated for 2080-2099 minus 1995-2014 for the
253 Australian continent and south-east Australia under SSP3-7.0 (for the latter, see Figure 3). The GCM
254 independence rankings were placed within this climate change space, with higher independence
255 rankings viewed as favourable, along with consideration of the following criteria:

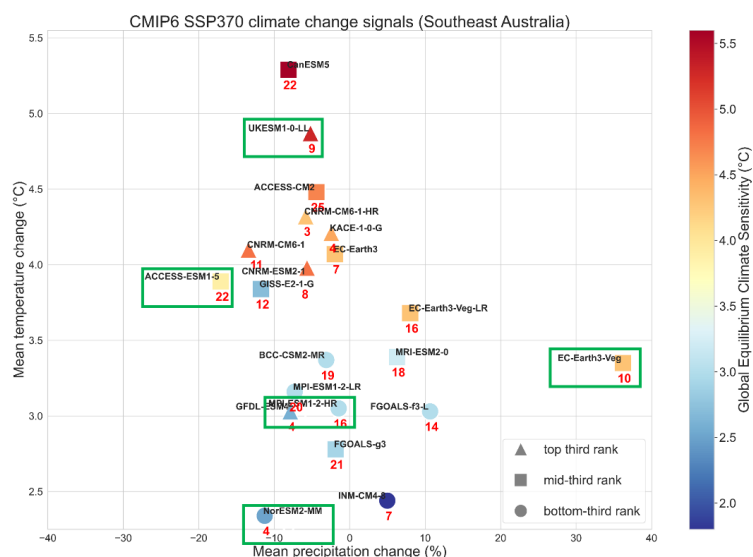
- 256 i) A balanced range of GCM Equilibrium Climate Sensitivities (ECS) were sampled. ECS is the
257 long-term increase in global mean surface air temperature in response to the radiative forcing
258 caused by a doubling of pre-industrial CO₂ concentrations. ECS is related to global tempera-
259 ture change, not just changes over Australia, however, it correlates strongly with regional
260 warming. Around one third of CMIP6 GCMs show ECS values higher than the upper end of
261 the likely range of 2.5°C to 4°C (IPCC, 2021). An upper range of > ~5°C cannot be ruled out
262 (Meehl et al., 2020; Bjordal et al., 2020; Sherwood et al., 2020).
- 263 ii) Some CMIP6 GCMs that are favourable in terms of model performance and independence
264 could not be selected as input to WRF for NARClIM2.0 owing to insufficient data availability
265 for key variables/variable, where ideally, WRF requires sub-daily data for the variables
266 shown in Supporting Information, Table S1.

267 As a result of the above process, the five CMIP6 GCMs listed in Table 2 are selected to force
268 NARClIM2.0 RCMs.



269 **Table 2.** Basic details of the CMIP6 GCMs used for NARcliM2.0 simulations.

CMIP6 GCM	Institution	Variant/Run	Atmosphere lat/lon grid (°)
ACCESS-ESM1-5	CSIRO	r6i1p1f1	1.2 × 1.8
EC-Earth3-Veg	EC-EARTH consortium	r1i1p1f1	0.7 × 0.7
MPI-ESM1-2-HR	Max Planck Institute for Meteorology (MPI)	r1i1p1f1	~0.9
NorESM2-MM	Norwegian Climate Centre	r1i1p1f1	0.9 × 0.9
UKESM1-0-LL	UK Met Office and NERC research centres	r1i1p1f2	1.3 × 1.9



270
 271 **Figure 3.** CMIP6 GCM climate change signals (2080-2099 versus 1995-2014) over south-east Australia for the
 272 subset of GCMs retained following the model performance evaluation in Di Virgilio et al. (2022), and that
 273 simulated at least monthly mean near surface air temperature and precipitation for the SSP-3.70 scenario. Boxed
 274 GCMs are selected to force NARcliM2.0 RCMs. Marker shapes indicate overall GCM performance; markers
 275 are coloured according to their global equilibrium climate sensitivity (ECS) values; **Red** numbers represent the
 276 smallest Herger Method 1 set for that GCM.

277 3.3 NARcliM2.0 RCM physics testing

278 The NARcliM2.0 RCM physics testing aims to identify and exclude RCMs that perform consistently
 279 poorly in simulating the southeast Australian climate and to select RCMs that have high statistical
 280 independence. The selection of RCMs in NARcliM2.0 involves the creation of a multi-physics
 281 ensemble where each RCM uses different physical parametrisations for PBL, microphysics, cumulus,
 282 radiation, and LSM. This enables many structurally different RCMs to be constructed and tested. In



283 NARClIM1.0, 36 WRF RCM configurations were designed, tested, and evaluated (Evans et al. 2014).
284 NARClIM2.0 physics testing assesses 78 RCM configurations which are progressively tested via three
285 phases, where each test phase is informed by the outcomes of the preceding phase to systematically
286 remove poor performing RCM options while facilitating the selection of parameterisations that
287 perform well during testing. The N=36 RCMs tested for NARClIM1.0 were evaluated based on eight
288 representative storm event simulations each of two-weeks duration (Evans et al. 2014). NARClIM2.0
289 physics simulations were run over an entire annual cycle (2016) with a two-month spin up period
290 commencing 1 November 2015. Australia experienced a range of weather extremes during 2016
291 driven by a range of climatic influences making 2016 a suitable target year (Bureau of Meteorology,
292 2017). Whilst assessing RCMs for an entire year improves on assessing for discrete storm events as
293 per physics testing for NARClIM1.0, it was not feasible to run a large RCM physics ensemble for a
294 longer duration. Initial and boundary conditions for all phases of the NARClIM2.0 RCM physics test
295 simulations were derived from the ERA-Interim reanalysis data set (Dee et al., 2011). ERA-Interim
296 was used because ERA5 was not available at the time. The three phases of NARClIM2.0 physics
297 testing are as follows:

298 **3.3.1 Phase I (N=36)**

299 Thirty-six RCMs were evaluated in Phase I. One radiation scheme (RRTMG) is tested for both long
300 and short-wave radiation (it is held fixed for all RCMs), whereas physics settings for PBL,
301 microphysics, cumulus, and LSM are varied. Of the 36 simulations, 18 used the Noah-Unified LSM,
302 whilst the remainder used Community Land Model version 4.0 (CLM4). The physics options tested
303 are listed in Table 3, where these were selected based on literature review. Each physics test
304 simulation is denoted by a 12-digit identifier which comprises 6 pairs of digits, with each pair
305 corresponding to the choice of a specific physics option as specified in the WRF namelist.input file.
306 These pairs of digits follow the order: planetary boundary layer (pbl) | cloud microphysics (mp) |
307 cumulus convection (cu) | shortwave radiation (sw) | longwave radiation (lw) | LSM (sf) and
308 correspond to the WRF namelist options shown in Table 3. For example, the simulation
309 ‘050601040402’ is interpreted as: 05 | 06 | 01 | 04 | 04 | 02 and denotes that this simulation uses the
310 following physics settings:

bl_pbl_physics	= 05 (MYNN2)
mp_physics	= 06 (WSM6)
cu_physics	= 01 (Kain-Fritsch)
ra_sw_physics	= 04 (RRTMG)
ra_lw_physics	= 04 (RRTMG)
sf_surface_physics	= 02 (Noah Unified)



311 The complete set of WRF RCM configurations tested in Phase I is shown in Supporting Information
312 Table S2.
313 **Table 3.** Physics options used in phase I (N=36) tests.

Physics Option Description	WRF Namelist	Options Tested
Planetary boundary layer	bl_pbl_physics	01 = YSU
		05 = MYNN2
		07 = ACM2
Microphysics	mp_physics	06 = WSM6
		08 = Thompson
Cumulus parameterisation	cu_physics	01 = Kain-Fritsch
		02 = BMJ
		06 = Tiedtke
Shortwave radiation	ra_sw_physics	04 = RRTMG
Longwave radiation	ra_lw_physics	04 = RRTMG
Land surface model	sf_surface_physics	02 = Noah-Unified
		05 = Community Land Model V4

314 **3.3.2 Phase II (N=60): additional LSM and radiation scheme tests**

315 Phase I RCMs using CLM4.0 were omitted from further testing because they did not consistently im-
316 prove performance in simulating the Australian climate relative to RCMs using Noah-Unified. In ad-
317 dition, RCMs using CLM4.0 had increased simulation times (by approximately twice when compared
318 to Noah-Unified). Hence, Phase II focuses exclusively on further testing of the RCM configurations
319 that used the Noah-Unified LSM.

320 The physics settings tested in Phase II are an alternative LSM to Noah-Unified (Noah Multi-
321 Parameterisation; ‘Noah-MP’, Niu et al., 2011) and New Goddard radiation. Owing to time/resource
322 constraints, testing all eighteen Phase I RCMs using Noah-Unified was not feasible. To reduce the
323 number of RCMs for further testing, the worst-performing Noah-Unified based RCM configurations
324 identified in Phase I were excluded. The N=18 RCMs using Noah-Unified are listed along with their
325 overall performance total scores in Table 4 where the lowest scores under ‘Rank totals’ indicate the
326 RCMs that overall perform relatively well versus their peers (see sect. 4 Evaluation Methods). Note
327 that the ‘Overall rank’ denotes the RCMs’ relative ranking among all Phase I RCMs. There is a sharp
328 reduction in rank totals for RCMs #13-18 inclusive, relative to RCMs #1-12. Therefore, RCMs #13-
329 18 are excluded from further testing, and RCMs #1-12 are retained.

330 **Table 4.** RCM physics combination ranks of the Phase I, N=18 Noah Unified (NU) based RCMs.
331 Scores/ranks are based on model bias and root mean square error for annual and seasonal precipita-
332 tion, minimum temperature, maximum temperature, climate extremes (wettest and hottest days), and
333 Perkins Skill Scores (see sect. 4). RCMs #1-12 are selected for further testing.



RCM #	RCM ID	Physics combination					Rank total	Overall rank in N=36 Phase I
		PBL	MP	Cumulus	SW/LW	LSM		
1	070801040402	ACM2	Thom	KF	RRTMG	NU	484	1
2	070601040402	ACM3	WSM6	KF	RRTMG	NU	495	2
3	070802040402	ACM4	Thom	BMJ	RRTMG	NU	527	3
4	070602040402	ACM5	WSM6	BMJ	RRTMG	NU	559	4
5	010802040402	YSU	Thom	BMJ	RRTMG	NU	574	7
6	050801040402	MYNN2	Thom	KF	RRTMG	NU	583	8
7	010801040402	YSU	Thompson	KF	RRTMG	NU	617	11
8	050802040402	MYNN2	Thompson	BMJ	RRTMG	NU	630	12
9	070606040402	ACM2	WSM6	Tiedtke	RRTMG	NU	639	13
10	050601040402	MYNN2	WSM6	KF	RRTMG	NU	662	16
11	070806040402	ACM2	Thompson	Tiedtke	RRTMG	NU	662	16
12	010602040402	YSU	WSM6	BMJ	RRTMG	NU	674	19
13	010601040402	YSU	WSM6	KF	RRTMG	NU	702	23
14	010606040402	YSU	WSM6	Tiedtke	RRTMG	NU	759	25
15	050606040402	MYNN2	WSM6	Tiedtke	RRTMG	NU	766	27
16	050602040402	MYNN2	WSM6	BMJ	RRTMG	NU	811	31
17	010806040402	YSU	Thompson	Tiedtke	RRTMG	NU	830	34
18	050806040402	MYNN2	Thompson	Tiedtke	RRTMG	NU	857	35

334 This gives two sets of physics combinations for additional testing: 1) one replaces only RRTMG
 335 (04|04) for short and longwave radiation with New Goddard (05|05) making no other changes; and
 336 2) RRTMG radiation is retained, but Noah-MP (04) replaces Noah-Unified (02). This creates an
 337 additional 24 RCM configurations for assessment, bringing the total RCMs tested to 60. Although
 338 Noah-MP has several parameter options, Phase II uses its default settings.

339 3.3.3 Phase III (N=78): parameterising Noah-MP

340 Phase II shows that RCM performance using New Goddard radiation is generally inferior to the same
 341 RCMs using RRTMG (see sect. 5. RCM Physics test results). Consequently, RRTMG radiation is re-
 342 adopted for Phase III. Conversely, a general performance improvement is conferred by using Noah-
 343 MP over Noah-Unified (sect. 5). Given this performance improvement using Noah-MP with default
 344 settings, Phase III assesses RCM performances using specific parameter settings for Noah-MP.

345 Noah-MP provides a ‘dynamic vegetation cover’ model option (referred to as dynamic vege-
 346 tation in the WRF users’ guide) (Niu et al., 2011). When deactivated (the default), monthly leaf area
 347 index (LAI) is prescribed for various vegetation types and the greenness vegetation fraction (GVF)
 348 comes from monthly GVF climatological values. Conversely, when dynamic vegetation cover is acti-



349 vated, LAI and GVF are calculated using a dynamic leaf model. We clarify here that dominant plant-
350 functional types do not change when using this option, but only the LAI and GVF, i.e. only the
351 amount of green cover changes.

352 Noah-MP also provides several options for modelling surface run-off and groundwater pro-
353 cesses including a TOPMODEL (TOPography based hydrological MODEL)-based surface runoff
354 scheme and a simple groundwater model (SIMGM; Niu et al., 2011). Some studies have shown using
355 this option improves modelling of soil moisture (e.g. Zhuo et al., 2019). Thus, three new sets of phys-
356 ics configurations are tested using Noah-MP where default options for specific settings are changed as
357 follows:

- 358 1. activate dynamic vegetation cover (dveg=2 in the WRF namelist); no other changes.
- 359 2. activate TOPMODEL runoff with simple groundwater (opt_run=1); no other changes.
- 360 3. activate both dynamic vegetation and TOPMODEL runoff with simple groundwater, no other
361 changes.

362 As above, the worst performing RCMs in Phase II are excluded from Phase III testing. Based
363 on the RCM configuration performance rankings (Table 5), there is a sharp reduction in performance
364 starting from RCM #7 inclusive. Therefore, RCMs #7-12 are excluded from further testing. Phase III
365 thus comprises 18 new test simulations (sets 1-3 each comprising 6 RCMs) bringing the total RCMs
366 tested to N=78. Phase III physics tests are denoted using the same RCM identification schemes distin-
367 guished by appending 'set_1', 'set_2', 'set_3' to identifiers.

368 **Table 5.** RCM physics combination ranks of the Phase II Noah-MP RCMs. Scores/ranks are based on model
369 bias and root mean square error for annual and seasonal precipitation, minimum temperature, maximum temper-
370 ature, climate extremes (wettest and hottest days), and Perkins Skill Scores (see sect. 4).

No.	Physics combination	Rank total
1	50801040404	721
2	70806040404	822
3	50802040404	848
4	70802040404	872
5	70601040404	880
6	50601040404	891
7	10802040404	988
8	70602040404	1005
9	70606040404	1028
10	10801040404	1042
11	70801040404	1056
12	10602040404	1264



371 **3.3.4 Shortlisting Physics Test RCMs for ERA5-NARClIM2.0 evaluation simulations**

372 Considering the complete NARClIM2.0 N=78 physics test ensemble, to identify physics test RCMs
373 that perform poorly overall, RCMs are eliminated if they are in the lowest 1/3 for RCM performance
374 ranks for any of maximum temperature, minimum temperature, precipitation, or for the overall model
375 performance rank across these variables (see sect. 5. RCM Physics test results). Under this scheme, 20
376 RCMs remain. The independence measures are then applied to the remaining 20 RCMs to choose a
377 final subset of 7 RCMs for ERA5-forced evaluation simulations (see sect. 3.4). The ensemble size
378 limit of N=7 is determined by available compute resources. These 7 candidate RCMs are assessed for
379 potential use in the CMIP6 GCM-forced downscaling phase of NARClIM2.0 (sect. 3.4 and Di Virgilio
380 et al. in review).

381 **3.4 CORDEX ERA5-NARClIM2.0 evaluation simulations**

382 NARClIM1.x performed production climate simulations using a two-phase process. Its RCM physics
383 testing selected definitive ‘production-grade’ RCMs which were then used to downscale both reanaly-
384 sis data and CMIP3/5 GCMs. In contrast, for NARClIM2.0, as described above the N=78 RCM phys-
385 ics testing culminates in shortlisting 7 ‘production-candidate’ RCMs which are used to downscale the
386 ERA5 reanalysis for 42-years (1979-2020). This enables assessment of shortlisted RCM performances
387 over a climatological period rather than the single year (2016) of the physics testing, which helps as-
388 certain that performance differences between shortlisted RCMs are robust across a multi-decadal
389 timescale capturing climatologically diverse years. The aim is that two definitive production-grade
390 RCMs can be selected for CMIP6-forced downscaling from these ERA5-forced CORDEX ‘evalua-
391 tion’ simulations. Thus, the seven ERA5-NARClIM2.0 RCMs were driven by ERA5.0 boundary con-
392 ditions for January 1979 to December 2020 using the model and nested domain setups described
393 above for NARClIM2.0. The skill of these RCMs in simulating the recent Australian climate was as-
394 sessed as follows (see Di Virgilio et al. in review): annual and seasonal means were calculated for
395 maximum and minimum temperature and precipitation using monthly means for temperature varia-
396 bles, and the monthly sum for precipitation. Extremes of maximum temperature and precipitation (99th
397 percentiles) and extreme minimum temperature (1st percentile) were calculated using daily data. RCM
398 performances in reproducing observations over these timescales were assessed by calculating model
399 outputs minus observations (i.e. model bias), and the RMSE of modelled versus observed fields. RCM
400 skill in simulating distributions of observed variables was assessed by comparing the probability den-
401 sity functions (PDFs) for daily mean observations versus those of the RCMs. The ultimate outcome of
402 these ERA5-forced simulations and their evaluation is the selection of two RCM configurations, R3
403 and R5 to run the CMIP6-forced phase of NARClIM2.0, see Di Virgilio et al. (in review) for further
404 details on the evaluation methods and results. Supporting Information Figure S1 shows the WRF
405 namelist settings for the R3 and R5 RCMs (see also sect. 9. Code Availability).



406 **3.5 CORDEX CMIP6-forced NARClIM2.0 simulations**

407 The ideal CMIP6 GCM variables and their frequencies required to run the WRF RCM are listed in
408 Table S1. A minority of variables in Table S1 are not available at sub-daily frequencies for every tar-
409 get GCM. This necessitates assumptions/data proxies to be made. For instance, soil moisture and soil
410 temperature variables were unavailable for some selected GCMs; hence, surrogate data, such as sur-
411 face temperature, were used for initialisation (noting that soil data are only used by the RCM at ini-
412 tialisation). In these cases, we investigated how long it took for uncertainty in the initial conditions to
413 disappear from the WRF output by analysing the regionally averaged soil moisture time series. The
414 data were regionalised according to the four Australian Natural Resource Management (NRM) re-
415 gions / climate zones (Supporting Information Figure S2) which are broadly aligned with climatologi-
416 cal boundaries (Fiddes et al., 2021) and with the IPCC reference regions (Iturbide et al., 2020). Time
417 series plots (Figure S3) show that soil moisture equilibrates to be within a normal range following
418 initialisation, indicating that the 12-month spin-up year (1950) is sufficient to account for the assump-
419 tions made at model initialisation.

420 Boundary and initial conditions were prepared using selected GCM data to run the 151-year
421 GCM-driven simulations using WRF version 4.1.2. The GCM-driven simulations were run and com-
422 pleted using the pre-defined RCM settings for two RCM configurations using the WRF namelists in
423 Supporting Information Figure S1 (see also sect. 9. Code Availability). A cold restart was performed
424 on the last Historical experiment year (2014), thus enabling the SSP1-2.6 and SSP3-7.0 experiments
425 to be run for 2015-2100 concurrently with the Historical experiment. The 2014 cold start year is even-
426 tually overwritten by Historical runs initiated in 1950.

427 **4. Evaluation methods**

428 This section largely focuses on the methods and metrics used for the NARClIM2.0 RCM physics test-
429 ing. Overviews of the methods and metrics for CMIP6 GCM evaluation and selection and assessments
430 of the ERA5-forced evaluation simulations are provided above, with further information on these
431 available in Di Virgilio et al. (2022) and Di Virgilio et al. (in review).

432 **4.1 Observations**

433 Australian Gridded Climate Data (AGCD version 1.0; Evans et al., 2020a) are the observational data
434 used to evaluate the NARClIM2.0 RCM physics test RCMs. These daily gridded data for maximum
435 and minimum temperature and precipitation are obtained from an interpolation of station observations
436 across Australia. AGCD data are on a regular WGS84 grid with a grid-averaged resolution of 0.05°.
437 For the NARClIM2.0 RCM physics tests, the AGCD data were re-gridded to correspond with the
438 RCM data from the inner domain on their native grids using a conservative area-weighted re-gridding



439 scheme. All data (RCM and AGCD) were restricted to a common extent contained within the inner
440 domain over southeast Australia, and a land mask was applied so that statistics were computed using
441 only land pixels. Treatment of AGCD for the CMIP6 GCM evaluation and the ERA5-NARClIM2.0
442 RCM evaluation is described in Di Virgilio et al. (2022) and Di Virgilio et al. (in review), respective-
443 ly.

444 **4.2 Methods and metrics: phase I-III physics tests**

445 RCM performances in reproducing observations for daily maximum and minimum temperature and
446 daily precipitation were assessed by calculating the model bias, i.e. model outputs minus AGCD, and
447 the RMSE of modelled versus observed fields. Model biases and RMSEs were calculated at annual
448 and seasonal timescales. The model representations of the hottest and the wettest day on an annual
449 time scale over the study region were also compared with AGCD. PDFs were calculated for each var-
450 iable using daily data. The Perkins skill score (PSS) (Perkins et al., 2007) was calculated to assess the
451 overall degree of overlap between modelled and observed distributions, with $PSS = 1$ indicating that
452 distributions overlap perfectly.

453 To identify the overall performances of the RCM configurations, the RCMs are ranked based
454 on the bias and RMSE for all variables and seasons, the annual PSS, as well as the bias and RMSEs
455 for the maximum temperature and precipitation extremes. These ranks are then summed with the low-
456 est totals indicating the best performing RCM configurations overall.

457 **4.3 CMIP6 GCM and ERA5-NARClIM2.0 evaluations**

458 Overviews of the evaluation methods and rationale for these components of NARClIM2.0 design have
459 been provided above. For further details on methods and results on the CMIP6 GCM evaluation and
460 the ERA5-NARClIM2.0 RCM evaluation, see Di Virgilio et al. (2022) and Di Virgilio et al. (in re-
461 view), respectively.

462 **4.4 Independence assessments**

463 We used the method of Bishop and Abramowitz (2013) as one of two methods of assessing the inde-
464 pendence of physics test RCMs and the target CMIP6 GCMs under evaluation for use in NAR-
465 ClIM2.0. This approach uses the covariance in model errors as the basis to define model dependence;
466 specifically, independence coefficients are derived from the error covariance matrix of the RCMs or
467 GCMs. Model independence is quantified using the correlation of model errors. For the physics test
468 RCMs, errors are computed by comparing the climatology of maximum and minimum temperature
469 and precipitation over the south-east Australia inner domain for 2016 with corresponding AGCD ob-
470 servations. The same calculation is performed for the CMIP6 GCMs, except for the Australian conti-
471 nent. Daily timeseries of precipitation, maximum and minimum temperature are calculated individual-



472 ly for each RCM and for AGCD. The simulated and observed daily timeseries of each variable are
473 then normalised by the standard deviation of the corresponding observed variable. These normalised
474 variables are concatenated for each RCM (GCM) and AGCD. An anomaly time series for each grid
475 cell is then produced. These time series are used to create a ‘model error covariance matrix’ contain-
476 ing the errors for all RCMs (GCMs). The coefficients of a linear combination of the RCMs (GCMs)
477 that optimally minimises the mean square error depends on both model performance and model de-
478 pendence (Bishop and Abramowitz, 2013). The result of this minimisation problem is written in terms
479 of the covariance matrix. The magnitude of coefficients assigned to each RCM (GCM) reflects a
480 combination of their performance and independence. Highly independent models have different errors
481 when simulating the recent climate. Models with the largest coefficients have the most independent
482 errors versus observations.

483 The Herger method of subset selection (Herger et al., 2018), as implemented here, uses quad-
484 ratic integer programming to find the subset of models whose equally-weighted subset mean (EWSM)
485 minimises a quadratic cost function. This cost function is chosen to measure the performance of the
486 EWSM in comparison to a given observational product. The two cost functions used here are: the
487 mean squared error (MSE) between the EWSM and the observational product (Herger et al. 2018, Eq.
488 1); and another which measures a combination of the MSE of the EWSM, the average MSE of each
489 subset member, and the average pairwise mean squared distance between subset members (Herger et
490 al. 2018, Eq. 2).

491 **4.5 NARClIM2 CMIP6-RCMs: historical evaluation and climate change** 492 **projections**

493 Performances of NARClIM2.0 versus NARClIM1.x RCMs in reproducing the recent Australian cli-
494 mate are evaluated by calculating the model biases (model outputs minus AGCD observations) for
495 mean maximum and minimum temperature and precipitation for 1990-2009. To enable comparison of
496 future projections between NARClIM1.0, NARClIM1.5 and NARClIM2.0 (where NARClIM1.0 mod-
497 elled for 1990-2009, 2020-2039, and 2060-2079), all NARClIM ensemble projected changes are
498 shown as far future (2060–2079) minus present day (1990–2009).

499 **4.6 Statistical significance**

500 When quantifying future climate change projections (compared to the historical period) and biases in
501 maximum and minimum temperature, the statistical significance is calculated for each grid cell using
502 t-tests ($\alpha = 0.05$) assuming equal variance. The Mann–Whitney U test is used for precipitation given
503 its non-normality. For individual RCMs, grid cells showing statistically significant changes are stip-
504 pled, otherwise they are shown in colour where change is statistically insignificant. Results on the
505 statistical significance of each ensemble mean are separated into three categories following Tebaldi et



506 al. (2011): 1) statistically insignificant areas are shown in colour, denoting that less than 50% of
507 RCMs are significantly biased/different; 2) in areas of significant agreement (stippled), at least 50%
508 of RCMs are significantly biased/different and at least 70% of significant models in the CMIP6-
509 NARCLiM2.0 RCM ensemble agree on the sign of the bias/difference. In such areas, many ensemble
510 members have the same bias sign which is an undesirable outcome; and 3) areas of significant dis-
511 agreement, where at least 50% of RCMs are significantly biased/different and fewer than 70% of sig-
512 nificant models agree on the bias sign, are shown with diagonal hatching for the CMIP6-NARCLiM2.0
513 historical evaluation and climate change signals.

514 **5. RCM Physics test results**

515 **5.1 Phase I RCM performance summary**

516 The spatial variation and magnitudes for Phase I RCM biases and RMSEs for annual mean maximum
517 and minimum temperature and precipitation are shown in Figures 4-5, respectively. Overall, RCMs
518 are biased cold for maximum temperature (mean absolute bias for the ensemble mean = 1.18 K), and
519 warm-biased for minimum temperature (mean absolute bias = 1.31 K; Figure 4a-b). Maximum tem-
520 perature RMSE magnitudes are large over the elevated terrain of the southeast coast and over western
521 regions (Figure 5a). The simulation of precipitation shows biases of varying sign, with wet biases that
522 are strongest over eastern coastal regions (Figure 4c). Precipitation RMSEs are particularly large
523 along the eastern coastline (>15 mm), and generally show an east-west gradient, i.e. progressively
524 decreasing further inland from the coast (Figure 5c).

525 **5.2 Comparing Phase II Physics Test RCM performances versus Phase I**

526 **5.2.1 Climate Means**

527 Overall, the RCM ensemble using New Goddard (NG) radiation has inferior performance to the corre-
528 sponding RCMs using RRTMG in terms of annual/seasonal mean maximum temperature biases,
529 RMSEs, and PSS (Table 7). In contrast, NG confers superior performance for annual/seasonal mean
530 minimum temperature for these statistics. RCMs using NG show reduced biases for annual mean and
531 spring-time precipitation, but larger errors for DJF and JJA (Table 7). RMSEs for annual and seasonal
532 precipitation are similarly variable.



533 **Table 7.** Climate means performance: phase II physics tests (i.e. N=12 set 1 changing only RRTMG to New
 534 Goddard (NG) and N=12 set 2 changing only land surface model (LSM) from Noah-Unified to Noah-MP
 535 (NMP) compared with the phase I physics test RCMs that were shortlisted for further testing (N=12).

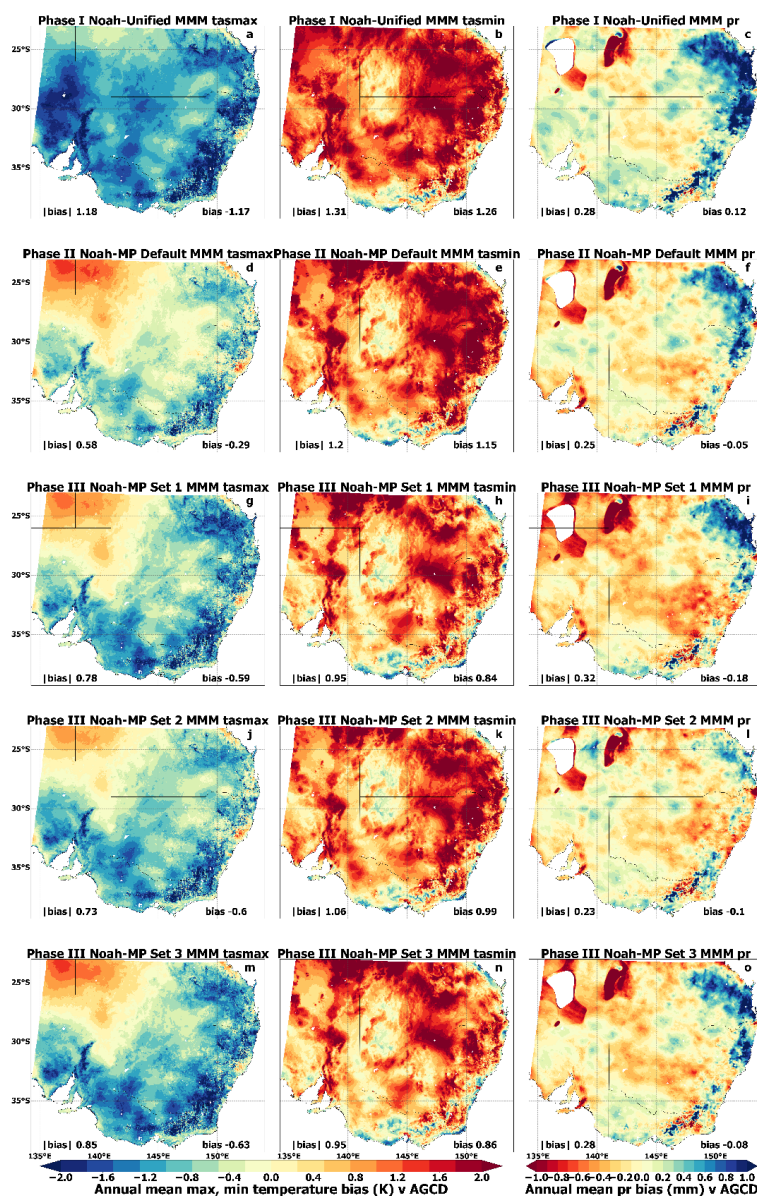
Variable	Timescale	Bias			RMSE			PSS		
		Phase I (N=12) ensemble mean	Phase II (NG rad.) ensemble mean	Phase II (NMP LSM) ensemble mean	Phase I (N=12) ensemble mean	Phase II (NG rad.) ensemble mean	Phase II (NMP LSM) ensemble mean	Phase I (N=12) ensemble mean	Phase II (NG rad.) ensemble mean	Phase II (NMP LSM) ensemble mean
Temp. Max. (K)	Annual	0.87	1.27	0.58	3.56	3.73	3.50	0.950	0.936	0.955
	DJF	0.74	1.29	0.63	4.41	4.70	4.43			
	MAM	1.40	2.06	0.83	3.68	3.92	3.55	-	-	-
	JJA	0.62	0.81	0.52	2.64	2.66	2.65			
	SON	0.87	1.04	0.66	3.25	3.32	3.20			
Temp. Min. (K)	Annual	1.35	0.95	1.2	3.53	3.41	3.42	0.927	0.941	0.931
	DJF	1.50	1.08	0.87	3.86	3.82	3.66			
	MAM	1.21	0.84	0.92	3.55	3.45	3.50	-	-	-
	JJA	0.82	0.51	0.91	3.00	2.92	3.00			
	SON	1.88	1.47	1.92	3.63	3.40	3.58			
Prec. (mm)	Annual	0.25	0.24	0.25	7.21	7.32	6.78	0.943	0.950	0.946
	DJF	0.41	0.53	0.49	8.28	8.83	8.85			
	MAM	0.32	0.32	0.25	5.91	6.47	5.53	-	-	-
	JJA	0.37	0.53	0.44	7.63	7.34	7.65			
	SON	0.34	0.22	0.39	6.68	6.18	6.92			

536 Phase II RCMs using Noah-MP with RRTMG retained show improved performance in simu-
 537 lating mean maximum and minimum temperature at annual timescales and most seasons relative to
 538 corresponding Phase I RCMs using Noah-Unified (Table 7; Figure 4-5). For instance, the mean abso-
 539 lute bias for annual mean maximum temperature is 0.58 K for the Noah-MP ensemble mean versus
 540 1.18 K for the Noah-Unified ensemble. In particular, cold bias magnitudes for maximum temperature
 541 are considerably lower over eastern and southern regions for the RCMs using Noah-MP (Figure 4d).
 542 RMSE magnitudes for maximum temperature are substantially reduced over the topographically com-
 543 plex regions of the southeast, and southwest and central regions (Figure 5d).

544 Overall, the magnitude of warm biases for minimum temperature are broadly similar for
 545 Phase I and Phase II RCMs (Figure 4b,c). Conversely, while RCMs in both Phases show large
 546 RMSEs for minimum temperature over several eastern regions, RMSEs are smaller for the Noah-MP
 547 ensemble over some southern areas (Figure 5b,c).



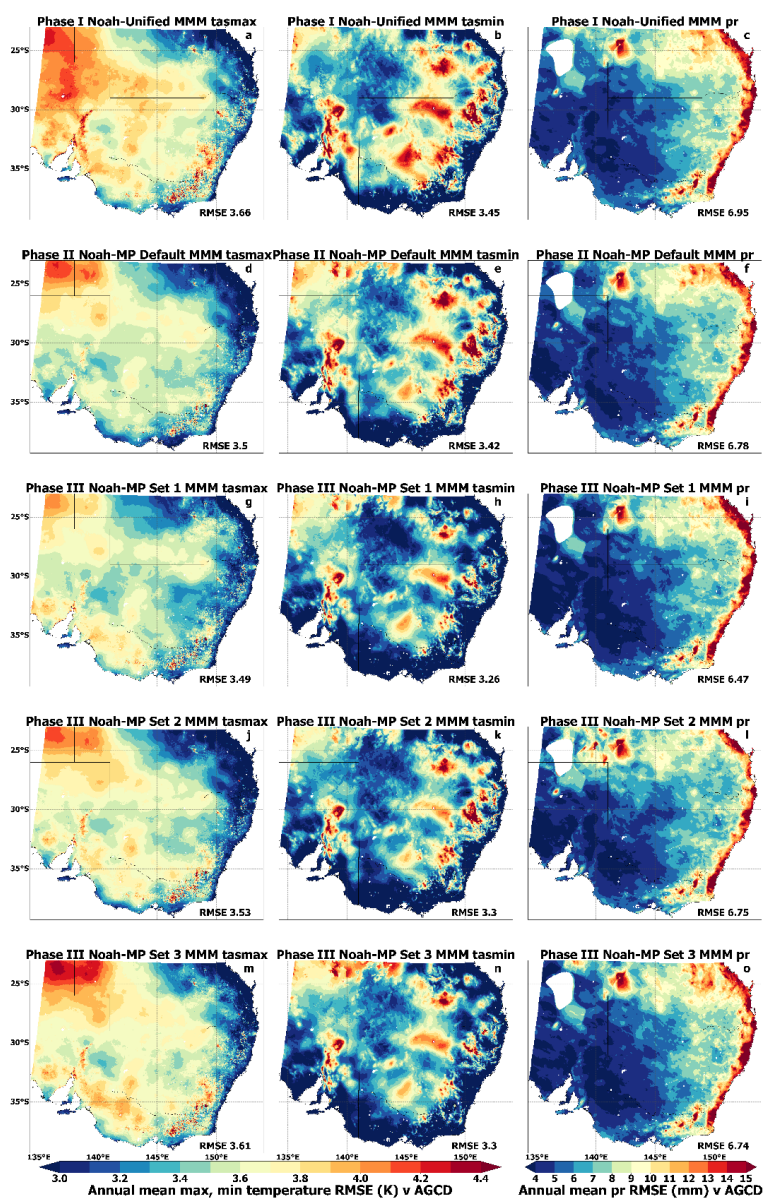
548 In contrast to the above results for the simulation of maximum temperature, overall, Phase II
 549 RCMs using Noah-MP show smaller performance improvements for the simulation of precipitation
 550 relative to the Phase I RCMs (Table 7). However, precipitation bias magnitudes are smaller for the
 551 Noah-MP ensemble over specific regions, e.g. north-eastern coastal regions and the elevated terrain of
 552 the south-east (Figure 4c,f).



553
 554 **Figure 4.** Phase I (N=36), Phase II (N=60) and Phase III (N=78) ensemble mean biases for annual mean maxi-
 555 mum temperature, minimum temperature and precipitation with respect to Australian Gridded Climate Data



556 (AGCD) observations for NARClIM2.0 Phase I physics test RCMs using Noah-Unified as the land surface
557 model (LSM) (a-c); Phase II physics test RCMs using Noah-MP as the LSM and its default settings (d-f); Phase
558 III 'set 1' physics test RCMs using Noah-MP with dynamic vegetation cover activated (g-i); Phase III 'set 2'
559 physics test RCMs using Noah-MP with TOPMODEL surface runoff and simple groundwater activated (j-l);
560 and Phase III 'set 3' physics test RCMs using Noah-MP with both dynamic vegetation cover and TOPMODEL
561 runoff activated (m-o).



562

563 **Figure 5.** As per Figure 4 but showing RMSEs.



564 **5.2.2. Climate Extremes**

565 Climate extreme analysis assesses RCM representations of the hottest and the wettest day versus
 566 AGCD. For both extremes and for RCM biases and RMSEs, Phase II RCMs using NG radiation
 567 showed inferior performance relative to phase I RCMs using RRTMG (Table 8). Conversely, Phase II
 568 RCMs using Noah-MP show substantial reductions in bias for both the hottest and wettest days (Table
 569 8). Phase II Noah-MP RCMs show a small increase in RMSE for the hottest day (Phase I bias=3.59
 570 K; Phase II bias=3.74 K); however, RMSEs are smaller for the wettest day (i.e. Phase I RMSE=19.20
 571 mm; Phase II RMSE=18.47 mm) (Table 8).

572 **Table 8** Climate extremes performance: comparing phase I RCMs (N=12) with phase II RCMs (i.e.
 573 12 RCMs changing radiation from RRTMG to New Goddard (NG) and 12 RCMs changing land sur-
 574 face model (LSM) from Noah-Unified to Noah-MP; NMP).

Variable	Bias			RMSE		
	Phase I (N=12) ensemble mean	Phase II (NG rad.) ensemble mean	Phase II (NMP LSM) ensemble mean	Phase I (N=12) ensemble mean	Phase II (NG rad.) ensemble mean	Phase II (NMP LSM) ensemble mean
Temp. max: hottest (K)	1.11	1.93	0.81	3.59	3.97	3.74
Prec.: wettest (mm)	3.08	3.21	2.60	19.20	20.52	18.47

575 **5.3 Phase III RCM performance summary and shortlisting N=7 RCMs for**
 576 **ERA5-NARClIM2.0 evaluation simulations**

577 Overall, RCM biases for mean maximum temperature do not show marked improvements once the
 578 dynamic vegetation cover and surface runoff options are activated for Noah-MP (Figure 4 g,j,m) rela-
 579 tive to RCMs using Noah-MP with default settings (Figure 4d). However, specifically for the RCM
 580 ensemble with dynamic vegetation cover activated for Noah-MP, RMSE magnitudes for maximum
 581 temperature are lower over some eastern coastal regions (Figure 5g).

582 The simulation of mean minimum temperature shows clear performance improvements for
 583 Phase III RCMs using options activated for Noah-MP, relative to RCMs using Noah-MP defaults.
 584 Overall, both biases and RMSEs for minimum temperature are reduced in magnitude for RCMs using
 585 the either or both of dynamic vegetation cover and runoff/groundwater options activated for Noah-



586 MP, relative to the default parameters (Figure 4-5). These performance improvements are largest over
587 eastern and southern regions.

588 There are no substantial overall performance improvements in the simulation of precipitation
589 for Phase III RCMs relative to Phase II RCMs (Figures 4-5 f,i,l,o). However, using Noah-MP with
590 specific LSM options remains favourable to using RCMs with Noah-Unified, albeit the performance
591 gains are generally small, except for some coastal regions and especially the north-east.

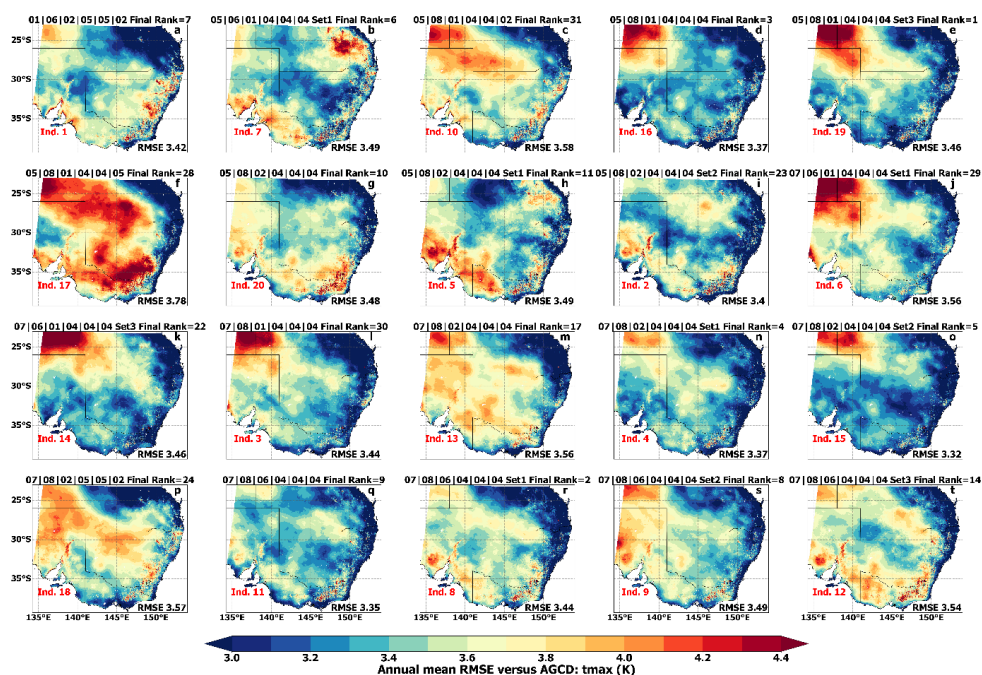
592 All 78 RCMs in the complete RCM physics test ensemble are ranked for performance as de-
593 scribed in sect. 4.2. Once the poor-performing RCMs are excluded, there are 20 RCMs remaining
594 (Table 9; Figures 6-8). In Table 9, we see that 16 Noah-MP-based RCMs from Phase II and Phase III
595 comprise this set of 20 RCMs, with 3 of the 20 RCMs using Noah-Unified, and 1 using CLM4.0. For
596 maximum temperature, some shortlisted RCMs show large RMSEs over north-western and inland
597 areas (e.g. Figure 6 d-f) that are of similar magnitude to those of the ensemble means of Phase I-III
598 RCMs (Figure 5). Conversely, several shortlisted RCMs show very low RMSEs for maximum tem-
599 perature across eastern and southern regions, especially along the eastern coast (Figure 6, e.g. RCMs
600 in panels d,l,n,o,q). For minimum temperature, a subset of the twenty shortlisted RCMs show substan-
601 tially reduced RMSEs over many regions relative to the Phase I-III ensemble means (Figure 7, e.g.
602 RCMs in panels: b,h,i). Additionally, several shortlisted RCMs show reduced RMSEs for precipita-
603 tion over the eastern coast and north-east (Figure 8, e.g. RCMs in panels: c, l, m, n, o) relative to the
604 Phase I-III RCM ensemble means in Figure 5c,f,i,l,o.

605 These 20 RCMs are assessed for statistical independence and 7 RCMs from this RCM set are
606 shortlisted for the ERA5-forced RCM simulations considering both their performance and independ-
607 ence scores (Table 9). These 7 shortlisted RCMs are listed in **bold** in Table 9 and are identified as R1-
608 R7 in the ERA5-forced evaluation simulations (Table 9; final column). RCMs are shortlisted from the
609 set of 20 if they rank highly for both performance and independence. For instance, RCM
610 050801040404_set_3 (top row, Table 9) is top-ranked for performance, however, its independence
611 scores/ranks are low, hence it is not shortlisted. It is important to note that, while a general perfor-
612 mance gain is observed in the physics testing when using Noah-MP, there are some specific RCM
613 configurations using Noah-Unified that perform well in simulating the Australian climate. For in-
614 stance, the RCM 010602050502 (row 7; Table 9; ‘R1’) uses Noah-Unified and performs well overall
615 (its overall performance rank=7), and especially for the simulation of maximum temperature (Figure
616 6a). It is also the only RCM in this set of 20 RCMs to use YSU for PBL. Importantly, this RCM is
617 highly ranked for statistical independence, hence, this RCM is shortlisted for the N=7 set.



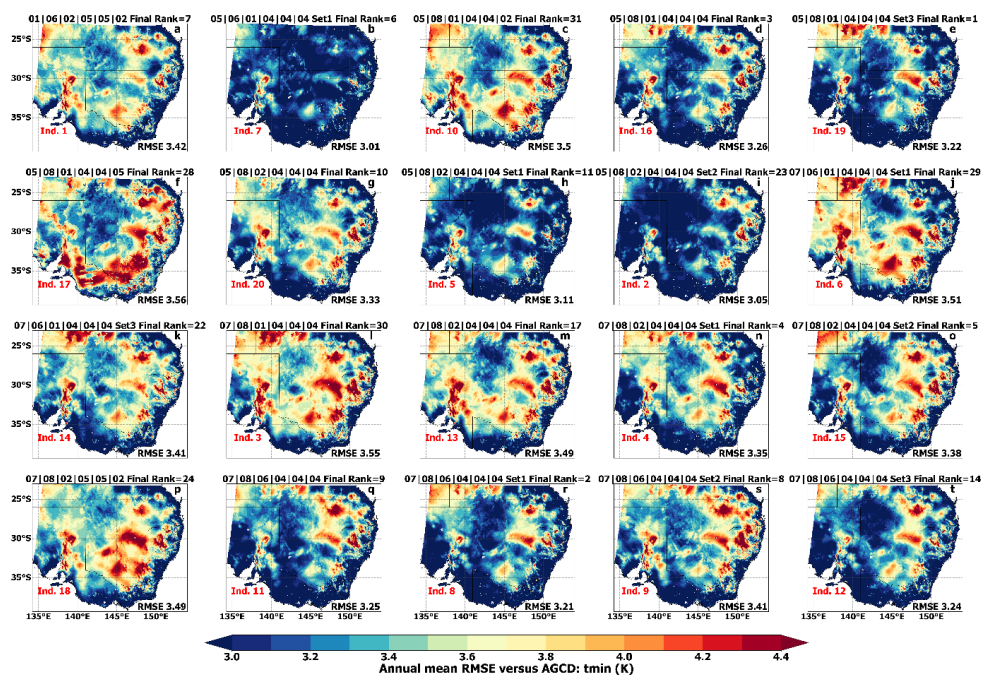
618 **Table 9.** The 20 NARClim2.0 physics test RCMs shortlisted from the full ensemble of 78 RCMs based on their
 619 performance in simulating the Australian climate and independence (Ind.) scores. N=7 ‘R1-R7’ RCMs shortlist-
 620 ed for ERA5-forced CORDEX evaluation simulations shown in **bold**. NU=Noah Unified; NMP=Noah-MP;
 621 DV=dynamic vegetation cover; TOP=topmodel runoff.

#	RCM Physics Combination	PBL	MP	Cumulus	SW/LW	LSM	Test Phase	Overall Performance Rank	Bishop Abramowitz Ind. Rank	Herger Ind. Set 1	Herger Ind. Set 2	ERA5-forced RCM Identifier
1	050801040404_set_3	MYNN2	Thom	KF	RRTMG	NMP DV+TOP	III	1	19	20	20	
2	070806040404_set_1	ACM2	Thom	Td	RRTMG	NMP DV	III	2	8	5	6	R6
3	50801040404	MYNN2	Thom	KF	RRTMG	NMP	II	3	16	12	13	
4	070802040404_set_1	ACM2	Thom	BMJ	RRTMG	NMP DV	III	4	4	3	3	R5
5	070802040404_set_2	ACM2	Thom	BMJ	RRTMG	NMP TOP	III	5	15	13	12	
6	050601040404_set_1	MYNN2	WSM6	KF	RRTMG	NMP DV	III	6	7	10	10	R2
7	10602050502	YSU	WSM6	BMJ	NG	NU	II	7	1	3	3	R1
8	070806040404_set_2	ACM2	Thom	Td	RRTMG	NMP TOP	III	8	9	9	5	R7
9	70806040404	ACM2	Thom	Td	RRTMG	NMP	II	9	11	14	14	
#	50802040404	MYNN2	Thom	BMJ	RRTMG	NMP	II	10	20	19	19	
#	050802040404_set_1	MYNN2	Thom	BMJ	RRTMG	NMP DV	III	11	5	2	2	R3
#	070806040404_set_3	ACM2	Thom	Td	RRTMG	NMP DV+TOP	III	14	12	10	10	
#	70802040404	ACM2	Thom	BMJ	RRTMG	NMP	II	17	13	15	15	
#	070601040404_set_3	ACM2	WSM6	KF	RRTMG	NMP DV+TOP	III	22	14	16	16	
#	050802040404_set_2	MYNN2	Thom	BMJ	RRTMG	NMP TOP	III	23	2	4	4	R4
#	70802050502	ACM2	Thom	BMJ	NG	NU	II	24	18	18	18	
#	50801040405	MYNN2	Thom	KF	RRTMG	CLM4	I	28	17	17	17	
#	070601040404_set_1	ACM2	WSM6	KF	RRTMG	NMP DV	III	29	6	7	8	
#	70801040404	ACM2	Thom	KF	RRTMG	NMP	II	30	3	1	1	
#	50801040402	MYNN2	Thom	KF	RRTMG	NU	I	31	10	6	7	



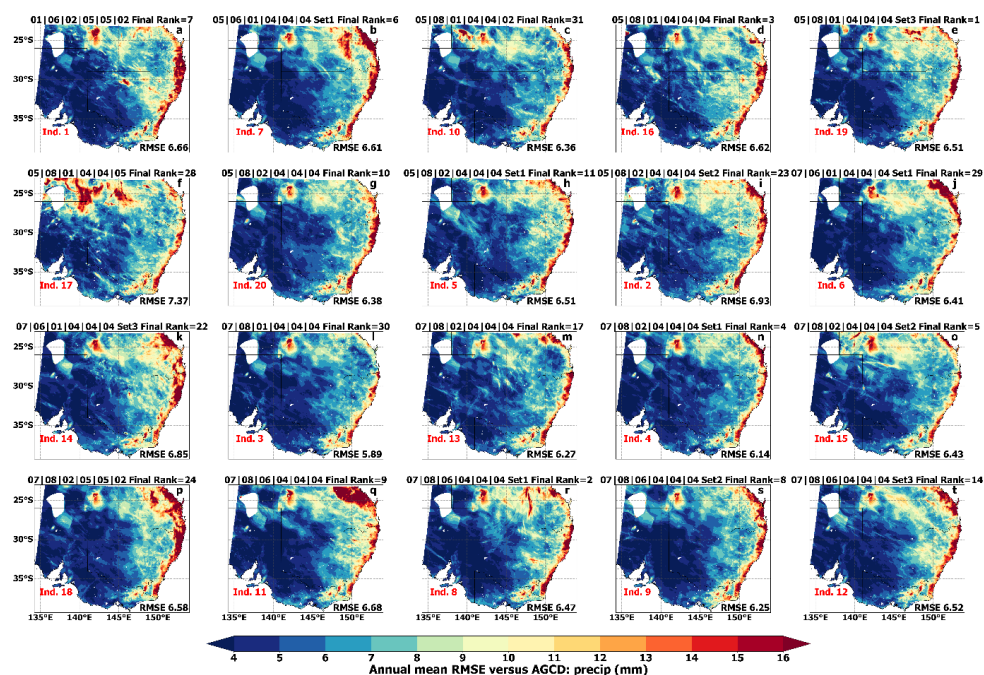
622

623 **Figure 6.** RMSEs for modelled mean maximum temperature (tmax) versus observations for the twenty
 624 NARClIM2.0 physics test RCMs shortlisted from the full ensemble of seventy-eight RCMs based on their
 625 performance in simulating the recent south-east Australian climate. Overall (final) performance ranks and
 626 Bishop and Abramowitz (2013) method independence (Ind.) scores are shown.



627
 628

Figure 7. As per Figure 6 but for mean minimum temperature (tmin).



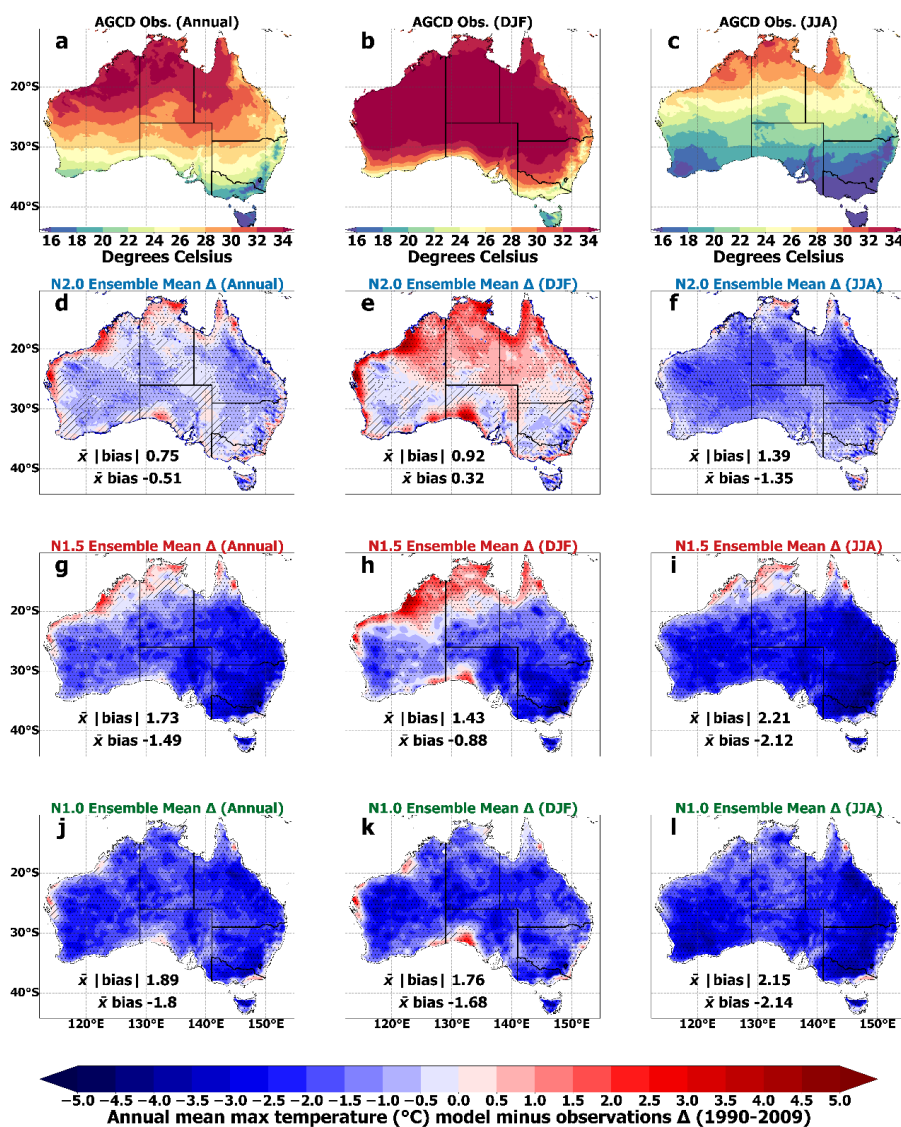
629

630 **Figure 8.** As per Figure 6 but for mean precipitation (precip.).

631 6. CORDEX-CMIP6 NARClM2.0 historical evaluation

632 6.1 Maximum temperature

633 NARClM2.0 RCMs simulate maximum temperature more accurately than NARClM1.x, with wide-
634 spread, statistically significant reductions in cold biases (Figure 9). These reductions in bias apply for
635 all timescales but are largest for the annual mean, i.e. the area-averaged mean absolute bias is 0.75°C
636 for the NARClM2.0 ensemble, 1.73°C for NARClM1.5, and 1.89°C for NARClM1.0 (Figure
637 9d,g,j). Notably, annual mean maximum temperature bias magnitudes are very small, i.e. around
638 <0.5°C, over south-west WA, southern coastal regions, and several eastern regions. This may be im-
639 portant from a climate change adaptation and mitigation perspective as these regions are heavily popu-
640 lated and economically significant. NARClM2.0 retains warm biases of similar magnitude to NAR-
641 ClM1.5 along the north-west coast of Australia (Figure 9d,g). Moreover, these warm biases cover
642 additional areas for NARClM2.0, especially during DJF (Figure 9e,h). A wide range of bias signs are
643 evident for the individual NARClM2.0 ensemble members (Figures S4-S6). The R5 RCM is general-
644 ly warmer than R3, e.g. (Figure S4c,d). Considering the forcing GCM data, overall, ensemble means
645 for the CMIP6 and CMIP5 GCMs generally show similar patterns and magnitudes of cold bias for
646 maximum temperature (Supporting Information S7).



647

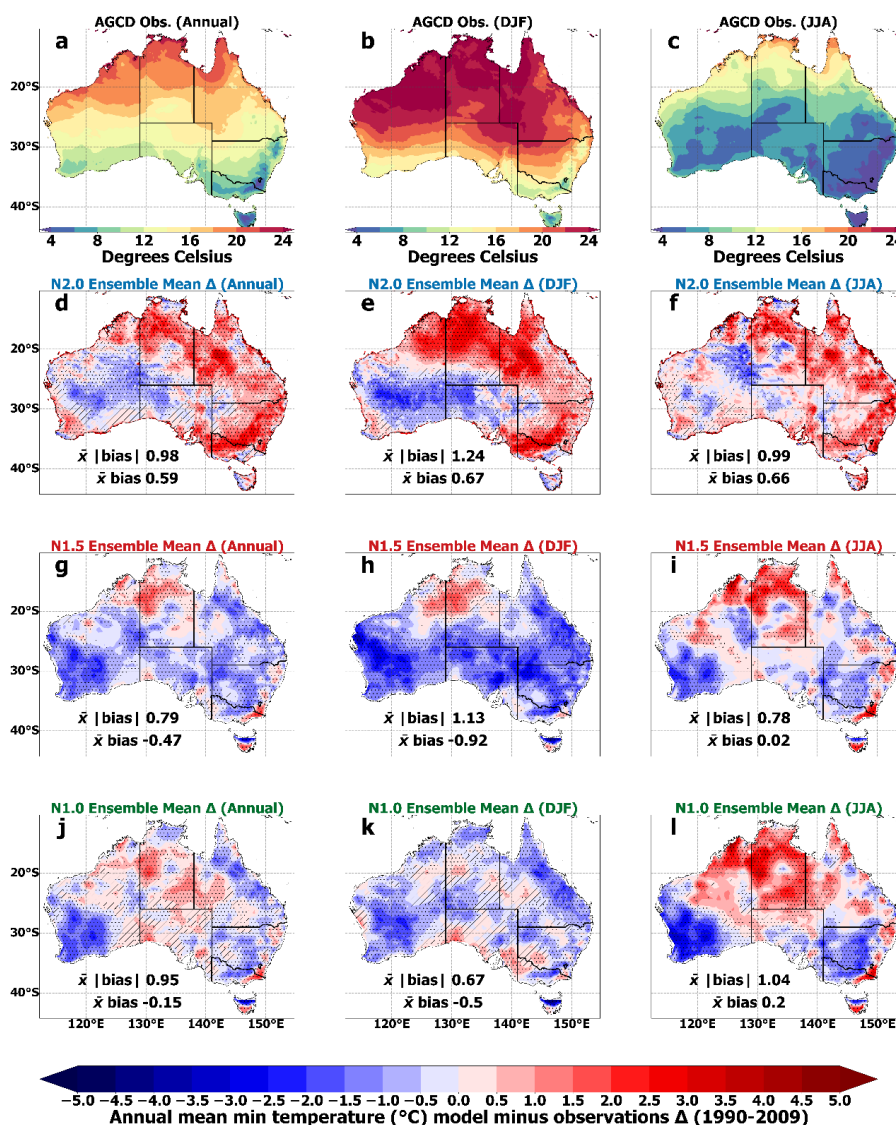
648 **Figure 9.** Annual, DJF and JJA mean near-surface atmospheric maximum temperature biases for NARClm2.0,
 649 1.5 and 1.0 historical ensemble means with respect to Australian Gridded Climate Data (AGCD) observations
 650 for 1990-2009. Stippled areas indicate locations where an RCM shows statistically significant bias ($P < 0.05$).
 651 Significance stippling for the ensemble mean bias follows Tebaldi et al. (2011) and is applied separately to each
 652 RCM ensemble. Statistically insignificant areas are shown in colour, denoting that less than half of the models
 653 are significantly biased. In significant agreeing areas (stippled), at least half of RCMs are significantly biased,
 654 and at least 70% of significant RCMs in each ensemble agree on the direction of the bias. Significant disagree-
 655 ing areas are shown in hatching, which are where at least half of the models are significantly biased and less
 656 than 70% of significant models in each ensemble agree on the bias direction - see main text for additional detail
 657 on the stippling regime.



658 **6.2 Minimum temperature**

659 The simulation of mean minimum temperature by NARcliM2.0 is generally warm biased at all time-
660 scales (Figure 10). Its bias magnitudes over many regions are larger versus NARcliM1.5, e.g. annual
661 mean area-averaged absolute biases are 0.98°C and 0.79°C for NARcliM2.0 and NARcliM1.5, re-
662 spectively (Figure 10 d,g). However, there are exceptions to this result over specific regions, for ex-
663 ample, parts of south-west western Australia show annual mean bias magnitudes of <1°C for NAR-
664 cliM2.0, but these areas show biases below -2°C for NARcliM1.x (Figure 10d,g,j). Most individual
665 RCMs comprising the NARcliM2.0 ensemble show stronger warm biases than their NARcliM1.5
666 peers at both annual and seasonal timescales (Figures S8-S10). The ACCESS-ESM-1-5-forced NAR-
667 cliM2.0 RCMs are considerably more warm-biased than the other NARcliM2.0 RCMs, with average
668 absolute biases of 1.74°C and 1.9°C; Fig. S8c-d).

669 Many of the CMIP6 GCMs used to force the NARcliM2.0 RCMs are warmer than the CMIP5
670 GCMs used to force NARcliM1.5, such that the ensemble mean bias of the former is 1.9°C versus
671 1.11°C (Figure S11). In particular, ACCESS-ESM-1-5 and MPI-ESM1-2-HR are substantially more
672 warm-biased relative to all other selected GCMs, with mean absolute biases of 2.2°C and 3.47°C, re-
673 spectively (Figure S11). This suggests that NARcliM2.0's warm biases for mean minimum tempera-
674 ture are at least partially inherited from the driving data. However, whilst the ACCESS-ESM-1-5-
675 forced NARcliM2.0 RCMs are much warmer than their counterparts (i.e. 1.74°C and 1.9°C), this
676 does not apply to the MPI-ESM1-2-HR-forced RCMs, which have biases of only 1.01°C and 1.09°C.
677 Hence, factors additional to the driving data, such as changes in RCM parameterisations between
678 NARcliM generations and other model design changes likely contribute to the warmer biases ob-
679 served for NARcliM2.0.



680

681 **Figure 10.** As per Figure 9 but for mean minimum temperature.

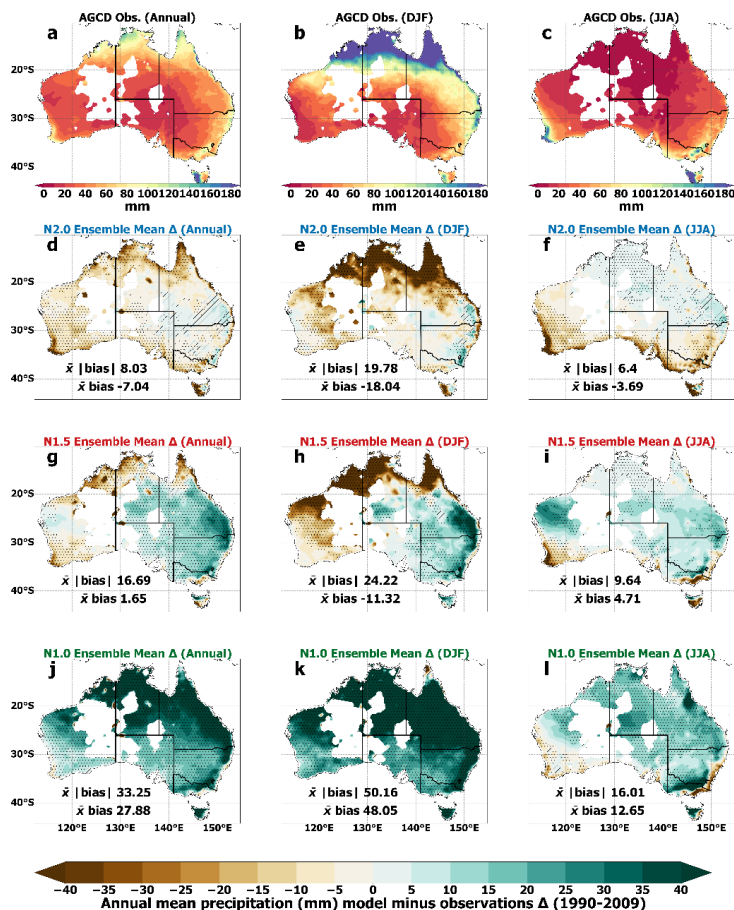
682 6.3 Precipitation

683 The NARClm2.0 ensemble shows small dry biases for mean precipitation over most regions, except
 684 for some areas mainly in the east of the country which show slight wet biases (Figure 11d-f). This
 685 contrasts with stronger, statistically significant wet biases of NARClm1.5 (Figure 11g-i) and the even
 686 stronger wet biases of NARClm1.0 (Figure 11j-l). Area-averaged bias magnitudes are considerably
 687 smaller for NARClm2.0 relative to NARClm1.x, especially for the annual mean, i.e. 8.03 mm ver-
 688 sus 16.69 mm and 33.25 mm, respectively. Annual mean precipitation biases are particularly small



689 over eastern regions, often being <5 mm. NARcliM2.0 retains the strong summertime dry biases for
 690 precipitation over northern Australia that are evident for NARcliM1.5 (Figure 11e,h), noting that this
 691 region also shows strong warm biases for maximum temperature (Figure 9).

692 The individual RCMs comprising NARcliM2.0 show a range of results for annual and sea-
 693 sonal mean precipitation biases (Fig S12-S14). Notably, three of the ten NARcliM2.0 RCMs have
 694 substantially larger bias magnitudes than their peers at annual and summer timescales, i.e. both MPI-
 695 ESM1-2-HR-R3 and R5 (absolute biases are 15.53 mm and 22.45 mm for annual mean precipitation,
 696 Figure S12g-h) and EC-Earth3-Veg-R5 (Figure S12f; 18.59 mm). Despite EC-Earth3-Veg-R5 being
 697 strongly dry-biased, EC-Earth3-Veg-R3 simulates precipitation more accurately i.e. its mean absolute
 698 bias=9.53 mm (Figure S12e). Analogously to NARcliM2.0's performances for temperature, R5 is
 699 drier than R3. Comparing the ensemble means of the driving GCMs, the CMPI6 GCMs are marginal-
 700 ly more accurate in simulating annual mean precipitation than the CMIP5 GCMs (Figure S15). Whilst
 701 the CMIP6 ensemble produces small biases over inland regions, its biases are larger along the east
 702 coast.

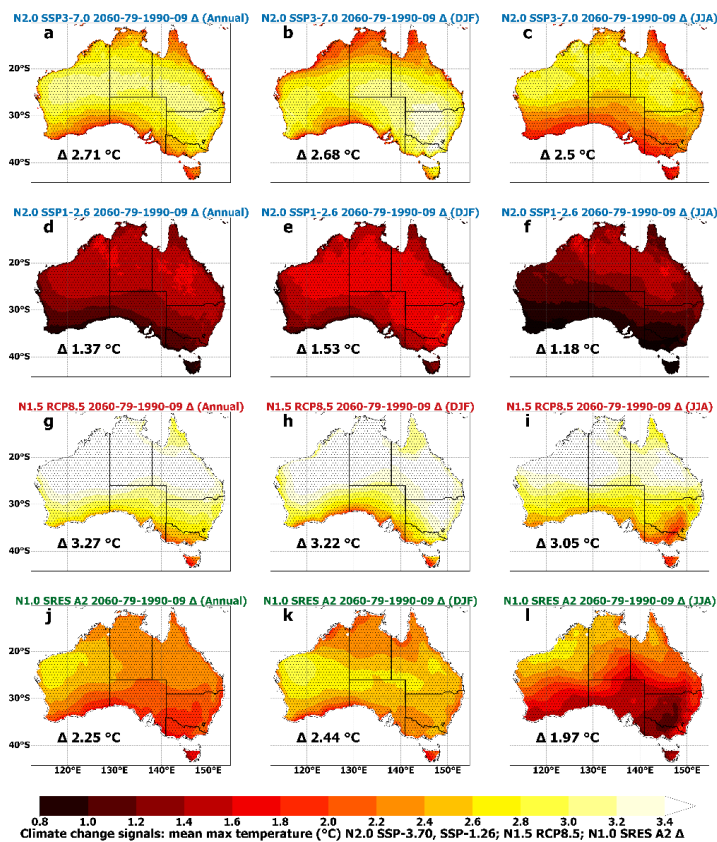


703
 704 **Figure 11.** As per Figure 9 but for mean precipitation (precip.).



705 7. CORDEX-CMIP6 NARClM2.0 climate change projections

706 Dependent on location, the largest maximum temperature projected increases for NARClM2.0 under
 707 SSP3-7.0 are over $\sim 3^\circ\text{C}$, and over $\sim 1.5^\circ\text{C}$ under SSP1-2.6 (Figure 12a,d). SSP3-7.0-NARClM2.0
 708 shows faster warming over inland than coastal regions, with greater warming across a horizontal band
 709 of the continent during annual and summer timescales (Figure 12a-b). This contrasts with NAR-
 710 ClM1.5 which shows a north-south warming gradient at annual and seasonal timescales, with its fast-
 711 est warming rate over northern regions, and NARClM1.0 which projects fastest warming over the
 712 west (Figure 12). For NARClM2.0, the tropical north warms faster during the winter dry season than
 713 during the summer wet season under SSP3-7.0, but this is not the case for SSP1-2.6 (Figure 12b-c; e-
 714 f). NARClM2.0 simulations under SSP3-7.0 show less warming than NARClM1.5-RCP8.5, but
 715 warmer futures than for NARClM1.0-SRES A2, with differences in the underlying driving GCMs
 716 and GHG scenarios likely contributing to these variations in warming. As per NARClM1.x, all
 717 NARClM2.0 maximum temperature projections are significant-agreeing with all RCMs projecting
 718 statistically significant temperature increases.

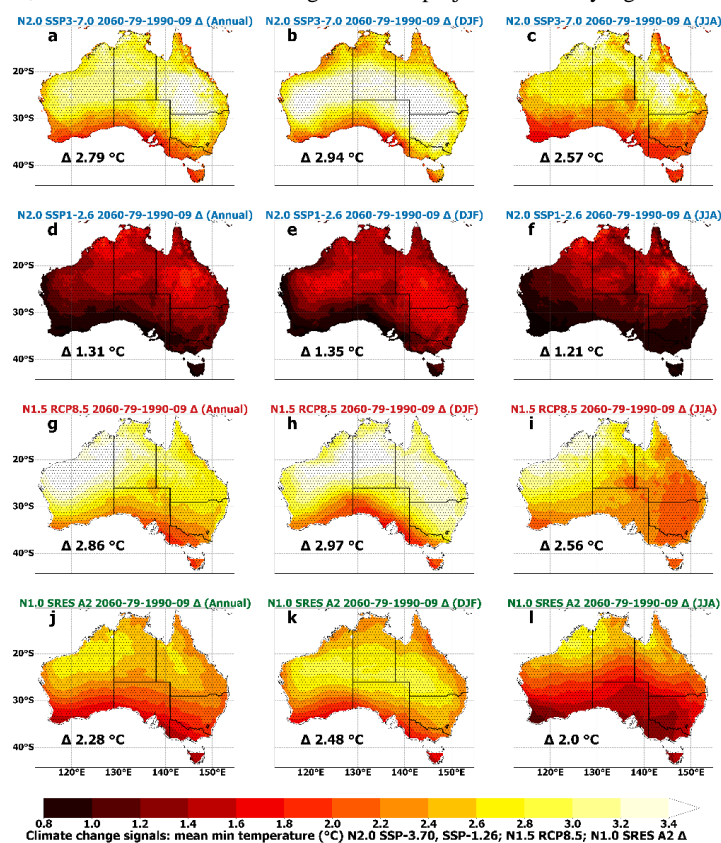


719

720 **Figure 12.** Ensemble mean climate change projections (far future minus present-day) for annual, DJF and JJA
 721 mean maximum temperatures with significance stippling as per Figure 9.



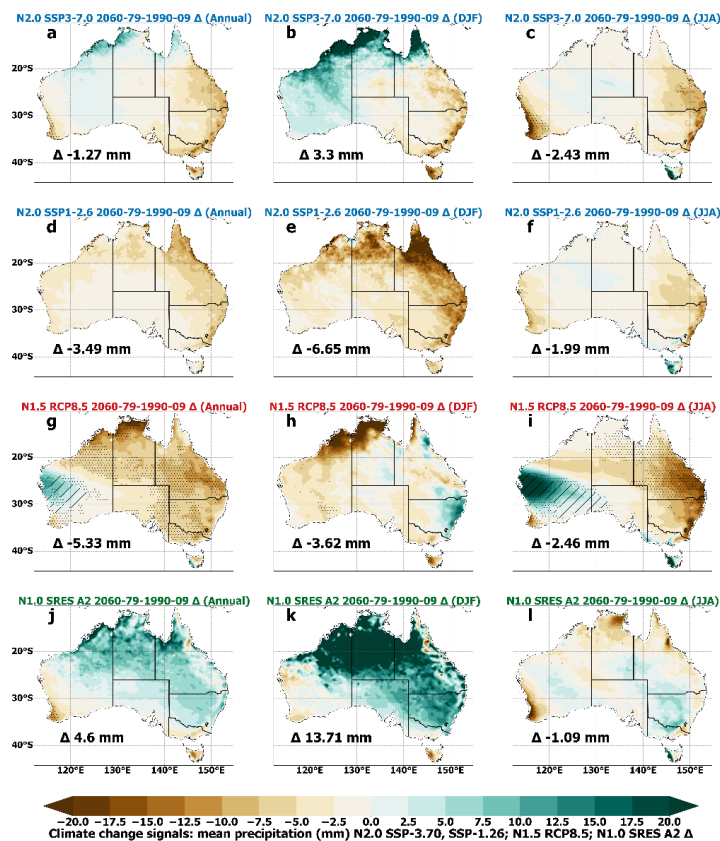
722 Projected increases in annual mean minimum temperature for NARClIM2.0 exceed 3°C over
723 some regions for SSP3-7.0, and 1.6°C for SSP1-2.6 (Figure 13). Under both GHG scenarios, at annual
724 and winter timescales warming is fastest over north-east Australia. Conversely, NARClIM1.x mini-
725 mum temperature future increases are generally largest over northwest or northern Australia, though
726 the summertime projection for NARClIM1.0 is an exception (Figure 13k). As for maximum tempera-
727 ture projections, all RCMs for all NARClIM generations project statistically significant increases.



728

729 **Figure 13.** Ensemble mean climate change projections (far future minus present-day) for annual, DJF and
730 JJA mean minimum temperatures with significance stippling as per Figure 9.

731 NARClIM2.0 SSP3-7.0 projects a dry future over most of Australia, except for wetter futures
732 over northern and western regions, which are largest in magnitude in summer (Figure 14a-b). In con-
733 trast, overall, NARClIM2.0 SSP1-2.6 projects dry changes across most of Australia, with the strongest
734 drying over northern Australia during summer (Figure 14e). Similarities between NARClIM2.0 pro-
735 jections for the low and high GHG SSPs include faster drying over the eastern coastline at all time-
736 scales, especially during summer. The wetter futures projected by RCMs downscaling SSP3-7.0-
737 GCMs relative to SSP1-2.6 may be partially inherited from the driving CMIP6 GCMs, because over-
738 all, SSP3-7.0 GCMs show wetter futures than corresponding SSP1-2.6 GCMs (Fig. S16).



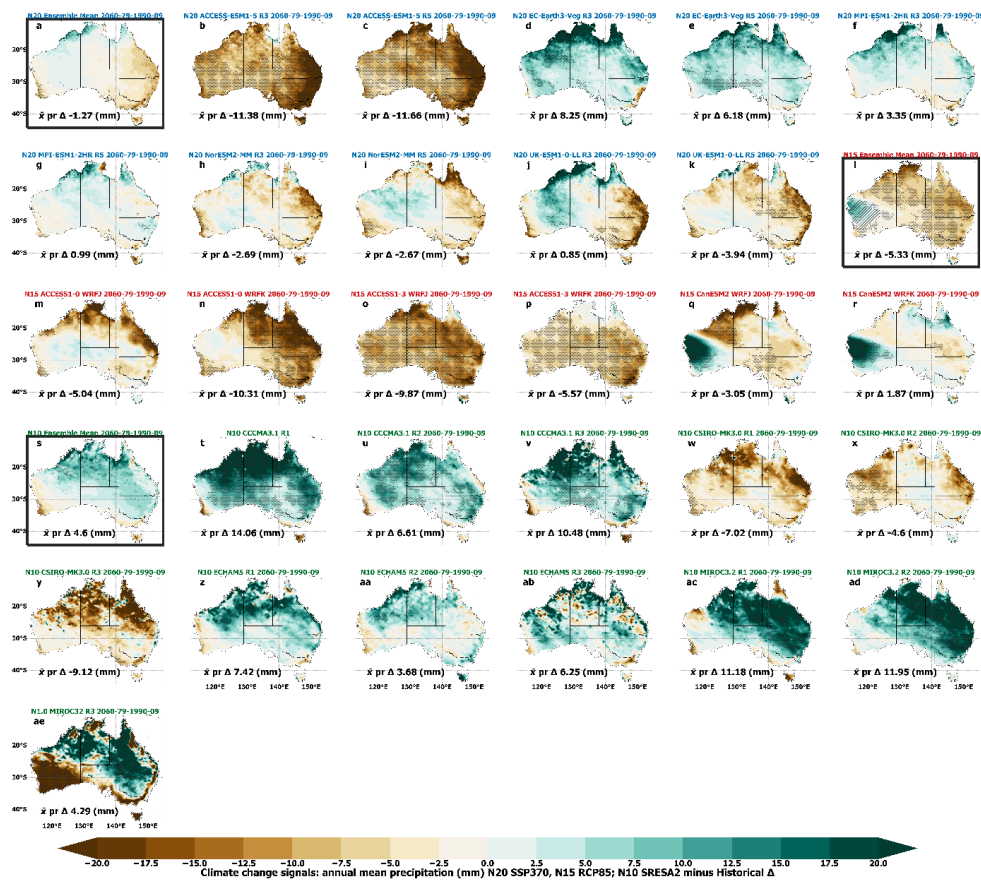
739
 740 **Figure 14.** Ensemble mean climate change projections (far future minus present-day) for annual, DJF and JJA
 741 mean precipitation with significance stippling as per Figure 9.

742 Considering mean precipitation projections for individual NARClIM2.0 RCMs, in some cases,
 743 R3 and R5 RCMs produce similar results when downscaling the same GCM. For instance, ACCESS-
 744 ESM-1-5 forced R3 and R5 both show statistically significant projected decreases in annual mean
 745 precipitation across Australia (Figure 15b-c). In contrast, while UK-ESM1-0-LL R3-R5 both show
 746 projected decreases in annual mean precipitation over eastern Australia, R3 shows precipitation in-
 747 creases that are substantially more widespread over western and northern regions relative to R5 (Fig-
 748 ure 15j-k). Overall, the NARClIM2.0 ensemble members show a variety of climate change signals for
 749 precipitation (Figure 15) and temperature (not shown), reflecting the range within the larger CMIP6
 750 ensemble (Di Virgilio et al. 2022).

751 There are some key differences between the mean precipitation projections of NARClIM2.0 rela-
 752 tive to those of previous NARClIM generations. For instance, NARClIM1.5 shows stronger reduc-
 753 tions in future precipitation over northern and eastern regions at annual and winter timescales (Figure
 754 14), and these changes are statistically significant over many regions, whereas there are only small
 755 regions of significant changes for NARClIM2.0. Additionally, NARClIM2.0 projects marked precipi-



756 tation decreases along the south-east coast during summer, while NARClIM1.5 shows the opposite
 757 result (Figure 14). NARClIM1.0 generally projects wet futures across larger portions of Australia,
 758 especially at annual and summer timescales.



759
 760 **Figure 15.** Climate change projections (1990–2009 versus 2060–2079) for annual mean precipitation for NAR-
 761 CliM ensemble mean climate change signals (a,l,s) and for individual ensemble members. Significance stippling
 762 as per Figure 9.

763 8. Discussion and Summary

764 NARClIM regional climate models produce robust climate projections at spatial scales suitable for
 765 local-scale climate change analysis and impact decision-making. The third and latest generation of
 766 these regional climate models, NARClIM2.0, encompasses several model design advancements over
 767 its predecessors.



768 **8.1 NARClIM2.0 RCM physics testing**

769 A key aim of this paper is to describe how NARClIM2.0 differs from its predecessors and explain the
770 rationale for these design decisions. In addition to RCM design choices including increased resolu-
771 tion, and incorporation of convection-permitting modelling and urban physics, a major change for
772 NARClIM2.0 relative to its predecessors is to use new WRF RCM configurations which are selected
773 via a large suite of physics tests. RCM performance evaluations for the NARClIM2.0 RCM physics
774 testing focused on the 4 km resolution convection-permitting domain which does not use a cumulus
775 physics parameterisation. Notably, the 7 ‘candidate’ shortlisted RCMs from the N=78 physics test
776 ensemble used three different cumulus parameterisations for their outer domains, with 4 RCMs using
777 BMJ, 2 RCMs using Tiedtke, and 1 using Kain-Fritsch. This indicates that differences in the outer
778 domain boundary conditions have key influences on the RCM performances in the convection-
779 permitting domain.

780 The use of the Noah-MP LSM in the NARClIM2.0 RCM physics tests conferred overall RCM
781 skill improvements relative to the test Phase I RCMs using the Noah-Unified LSM, especially in
782 terms of the simulation of temperature. Although using Noah-MP also improved the simulation of
783 precipitation in some respects, these improvements were smaller relative to the gains for temperature,
784 and improvements were mainly located over coastal regions. The developers of Noah-MP suggest that
785 some limitations in the Noah-Unified LSM have been modified to better represent several parameters.
786 These include surface layer radiation balances, snow depth, soil moisture and heat fluxes, leaf area-
787 rainfall interaction, vegetation and canopy temperature distinction, drainage of soil, and runoff.

788 In the NARClIM2.0 physics testing, improvements in RCM skill were evident for Noah-MP
789 with default settings. Activating specific parameterisations for this LSM (i.e. dynamic vegetation cov-
790 er and surface runoff-simple groundwater) delivered comparatively smaller gains in RCM perfor-
791 mances. Some previous studies have found no overall benefit of using Noah-MP with default settings.
792 For instance, Imran et al. (2018) conducted an evaluation of WRF coupled with a variety of LSMs
793 including Noah-MP using its default settings. Their focus was on simulating short-duration (~3-day)
794 heatwaves in Melbourne, Australia. They observed larger temperature biases using Noah-MP relative
795 to RCMs using Noah-Unified and CLM4.0. However, their focus on specific heatwave events of short
796 duration over one urban area was not intended as a comprehensive evaluation of Noah-MP’s perfor-
797 mance using default settings over longer timescales. It is also important to consider that several phys-
798 ics schemes used by these authors differed to those used in the NARClIM2.0 physics testing, i.e. they
799 used: PBL=MYJ; microphysics=Thompson; cumulus=Grell3D; radiation=RRTMG/RRTMG. The
800 only similarities between these settings and those of the NARClIM2.0 physics testing are the use of
801 Thompson microphysics and RRTMG. WRF and Noah-MP versions also differed, i.e. Imran et al.
802 used WRF3.6.1 and a Noah-MP version prior to 3.7, whereas NARClIM2.0 uses WRF4.1.2 and No-
803 ah-MP version 4.1.



804 In an assessment of the performances of several WRF-LSMs for Sub-Saharan Africa, Glotfelty et
805 al. (2021) noted deficiencies in the simulation of land use and land cover change (LULCC) param-
806 eters such as surface albedo by Noah-MP. Despite these deficiencies, the spatial patterns and magni-
807 tudes of temperature and precipitation were well-represented by Noah-MP. However, the land surface
808 parameter errors impacted the magnitude and sign of LULCC-induced changes in temperature and
809 precipitation. These deficiencies were linked to substantial underestimations of surface albedo in arid
810 areas due to inaccurate soil albedo treatments by Noah-MP. Moreover, errors in Noah-MP's LAI pro-
811 files may occur because it was developed principally for application in Northern Hemisphere mid-
812 latitudes. It is possible that modifying/tuning Noah-MP to specific aspects of the Australian context
813 would yield performance benefits for follow-up dynamical downscaling. Overall, these authors con-
814 cluded that "Noah-MP is least flawed of the [WRF] default LSMs". Additionally, there are also sever-
815 al studies that have reported benefits of using Noah-MP with default parameters relative to other
816 LSMs e.g. Chen et al. (2014b), Chen et al. (2014a) and Salamanca et al. (2018).

817 The NARClIM2.0 physics testing found that the optimal LSM configuration for simulation of
818 minimum temperature used Noah-MP with dynamic vegetation cover activated, even though the per-
819 formance gain relative to Noah-MP with default settings was small. Constantinidou et al. (2020) ran
820 WRF coupled with four LSMs (Noah-Unified, Noah-MP, CLM and, Rapid Update Cycle) over Mid-
821 dle East North Africa CORDEX domain. Their study compared the performance of Noah-MP with
822 dynamic vegetation cover turned on and off. They showed that air and land temperatures were best
823 simulated using Noah-MP with dynamic vegetation cover activated.

824 Overall, Noah-MP performed well in the NARClIM2.0 physics tests, conferring some clear ad-
825 vantages over RCMs using Noah-Unified. However, given the nature of its development and perfor-
826 mance characteristics, it may be more suited to application over the temperate regions of Australia
827 rather than the semi-arid interior.

828 In terms of PBL parameterisations, by the completion of Phase I physics testing, only 3 of 12
829 RCMs shortlisted for further testing use the YSU scheme. By the completion of Phase II testing, all
830 remaining RCMs using YSU are discarded, with only RCMs using PBL schemes other than YSU re-
831 maining (i.e. ACM2 and MYNN2). YSU PBL is a first-order closure scheme that expresses turbulent
832 mixing via mean variables rather than prognostic variables (Hong et al., 2006). It is classed as a 'non-
833 local' scheme because it estimates turbulent mixing by small-scale eddies as well as representing
834 transport caused by convective large eddies. Two previous studies evaluating convection permitting
835 WRF simulations using different parameterisations that included YSU for the PBL scheme found that,
836 relative to other PBL schemes, YSU produced the highest bias for simulated precipitation (Huang et
837 al., 2023; Nuryanto et al., 2019). However, these studies focused on different regions globally, and
838 used various experimental setups that are not directly comparable to those used here. Hence, a sepa-
839 rate study investigating sensitivities of the NARClIM2.0 RCMs to the different PBL schemes is cur-
840 rently underway.



841 **8.2 CMIP6-NARClIM2.0: historical evaluation and climate change** 842 **projections**

843 We characterised the improvements conferred by NARClIM2.0 over its predecessors in simulating the
844 present-day Australian climate. NARClIM2.0 simulates mean maximum temperature and precipitation
845 more accurately than NARClIM1.x. Specifically, NARClIM1.x has strong maximum temperature cold
846 biases which are in keeping with other downscaling projects of the CMIP3-CMIP5 eras, e.g. (Andrys
847 et al., 2016; Evans et al., 2020b), but these are substantially reduced in NARClIM2.0. A contributing
848 cause of CMIP5-forced RCM cold biases of maximum temperature is their overestimation of precipi-
849 tation (Evans et al., 2020). This relationship was also noted in ERA-Interim forced RCMs of this
850 modelling era (Di Virgilio et al. 2019). In NARClIM2.0, the widespread wet biases that characterise
851 the NARClIM1.x RCMs are greatly reduced in magnitude. NARClIM2.0 produces smaller wet biases
852 over eastern Australia, and smaller dry biases elsewhere, except for Australia's tropical north. This
853 marked reduction in wet bias magnitudes is a plausible contributing cause for the reduction in maxi-
854 mum temperature cold bias for the NARClIM2.0 RCMs. The CMIP6 and CMIP5 GCMs used to drive
855 NARClIM2.0 and 1.5 RCMs generally show similar magnitudes of maximum temperature cold bias.
856 This suggests that the underlying nature of the CMIP6 driving data is not a principal factor underlying
857 the observed improvements for NARClIM2.0's simulation of maximum temperature. In fact, the
858 RCMs appear to have a substantial influence on the reduced maximum temperature biases.

859 That NARClIM2.0 underestimates precipitation over tropical northern Australia during the
860 wet season (summer) to a similar degree of magnitude to the NARClIM1.5 RCMs indicates that the
861 newer models still struggle to accurately capture the strength of the Australian monsoon. However,
862 whereas NARClIM1.x strongly overestimates precipitation over south-eastern and southern Australia,
863 wet biases over these regions are reduced for NARClIM2.0 RCMs. This indicates that the newer mod-
864 els may confer an improved simulation of broad-scale processes associated with synoptic-scale sys-
865 tems interacting with the extratropical storm track over Australia (Grose et al., 2019).

866 NARClIM2.0 RCMs overestimate minimum temperatures across Australia, and these biases
867 are larger relative to NARClIM1.5 but comparable to those of NARClIM1.0. The CMIP6 GCMs used
868 to force NARClIM2.0 show substantially stronger warm biases for minimum temperature than the
869 CMIP5 GCMs used for NARClIM1.5. This suggests that the increased warm bias for minimum tem-
870 perature in NARClIM2.0-RCMs is partially inherited from the driving GCMs. However, as noted
871 above, the Noah-MP LSM simulation of factors such as LAI and other aspects of vegetation as well as
872 surface albedo in arid areas may contribute to the biases shown by the NARClIM2.0 RCMs. Moreo-
873 ver, the NARClIM2.0 ensemble mean reduces the overall minimum temperature bias of the CMIP6
874 GCM ensemble by almost half, attesting to the added value conferred by the NARClIM2.0 RCMs
875 with respect to near-surface temperature variables.



876 In terms of NARClIM2.0 future climate projections, major changes between NARClIM genera-
877 tions such as differences in GHG scenarios mean that NARClIM2.0 projected temperature changes
878 differ in some respects to those of its predecessors. Overall, as is expected, projected warming is less
879 intense in NARClIM2.0 under SSP3-7.0 than for NARClIM1.5 under RCP8.5. Other differences in
880 the projections between NARClIM generations require further investigation in order to explain, such
881 as NARClIM1.5's latitudinal warming gradient for maximum temperature that contrasts with NAR-
882 ClIM2.0's band of faster warming over central Australia relative to northern and southern regions.
883 Irrespective of these differences, all three NARClIM ensembles show statistically significant-agreeing
884 results for warming projections.

885 Precipitation projections for the different NARClIM generations show some key similarities,
886 such as reductions in mean annual precipitation over eastern Australia for NARClIM2.0 and NAR-
887 ClIM1.5, though a difference is that these are statistically significant only for NARClIM1.5. The
888 NARClIM2.0-SSP3-7.0 and SSP1-2.6 ensembles differ in that the former generally projects wet
889 changes over northern and western Australia, whereas the latter is generally dry, results that appear
890 partially traceable to the underlying driving CMIP6-SSP data. Other notable differences are that some
891 NARClIM2.0 RCMs produce very similar precipitation projections for certain GCM-RCM combina-
892 tions, such as for ACCESS-ESM-1-5 forced R3 versus R5 under SSP3-7.0 (i.e. widespread dry pro-
893 jections for both RCMs). Conversely, in other instances, there are marked divergences between the R3
894 versus R5 precipitation projections when forced with the same GCM, for instance, UK-ESM-1-0-LL
895 under SSP3-7.0 where R3 projects stronger precipitation increases that are more geographically wide-
896 spread relative to R5. This raises the question of varying sources of uncertainty in the climate projec-
897 tions, i.e. to what extent these are attributable to GCMs versus RCMs, as well as other factors.

898 In summary, the CORDEX-CMIP6 NARClIM2.0 regional climate projections are a 10-member
899 ensemble comprising two configurations of the WRF RCM dynamically downscaling five GCMs un-
900 der three SSPs at 20 km resolution over CORDEX-Australasia and at 4 km convection-permitting
901 resolution over south-east Australia. The main aims of this manuscript are to describe the new
902 CORDEX-CMIP6 NARClIM2.0 RCM ensemble, explaining how and why its design choices were
903 made including the model test and evaluation approaches underlying these design decisions; and char-
904 characterise improvements in model skill in simulating the recent Australian climate relative to previous
905 generations of NARClIM, as well as differences in future climate projections. In addition to several
906 high-level model design changes, e.g. increased spatial resolution, a large (N=78) RCM-physics test
907 suite is evaluated to select two new WRF RCM configurations for CMIP6-forced NARClIM2.0 cli-
908 mate projections. Due to resource constraints and the aim to test a large number of RCM physics pa-
909 rameterisations, the NARClIM2.0 physics tests are performed for a single year. This is one reason
910 why the final selection of two production-grade RCMs for the CMIP6-NARClIM2.0 runs is based on
911 the CORDEX ERA5-forced 42-year evaluation simulations. The NARClIM2.0 physics tests identified
912 RCM configurations that generally performed well in simulating the recent Australian climate over



913 southeast Australia. A key finding was that WRF RCMs using the Noah-MP LSM generally out-
914 performed RCMs using other WRF LSMs in representing regional climate. Despite the performance
915 gains evident for RCMs using Noah-MP, RCM skill was superior over the temperate/coastal regions
916 of southeast Australia, relative to the semi-arid interior. These performance characteristics might be
917 linked to Noah-MP's development being focused on Northern Hemisphere mid-latitudes, including
918 assumptions such as accounting for differences in seasonality in the Northern versus Southern Hemi-
919 spheres by shifting the Northern Hemisphere LAI profiles by 6 months. For the southeast Australian
920 context, noting its distinctive coastal dry-sclerophyll and expansive inland grassland biomes, such
921 assumptions might lead to discontinuities in quantities such as LAI. Hence, future investigation into
922 processes such as land-surface coupling in NARClIM2.0 RCMs is warranted.

923 Overall, the CMIP6-NARClIM2.0 ensemble produces a good representation of recent mean cli-
924 mate that in several key respects improves upon the model skill of earlier NARClIM generations. This
925 study provides a foundation for more detailed investigations of the model biases and future climate
926 changes described here, including process-focused studies exploring their mechanisms. CORDEX-
927 CMIP6 NARClIM2.0 RCM data provide valuable resources to investigate projected climate changes,
928 their impacts on societies and natural systems, and potential climate change mitigation and adaptation
929 actions for the CORDEX-Australasia region.

930 **9. Code Availability**

931 The Weather Research and Forecasting (WRF) version 4.1.2 used in this study is freely available
932 from: <https://github.com/coecms/WRF/tree/V4.1.2>. A static copy of all scripts used for this study can
933 be found at: [https://bitbucket.org/oeucas/narclim2-
934 0_design_and_evaluation_2024_support_materials/src/main/](https://bitbucket.org/oeucas/narclim2-0_design_and_evaluation_2024_support_materials/src/main/)

935 **10. Data Availability**

936 Data for the NARClIM2.0 CMIP6-forced R3 and R5 RCMs are being made available via [National](#)
937 [Computing Infrastructure](#) (NCI). WRF namelist settings for the NARClIM2.0 CMIP6-forced R3 and
938 R5 RCMs are shown in Supplementary Material Figure S1 and are also available at:
939 https://bitbucket.org/oeucas/narclim2-0_design_and_evaluation_2024_support_materials/src/main/.
940 Data NARClIM1.5 RCMs are available via the [New South Wales Climate Data Portal](#) and [CORDEX-
941 DKRZ](#). Data for NARClIM1.0 RCMs are available via the [New South Wales Climate Data Portal](#).
942 CMIP6 GCM data are available via the [Earth System Grid Federation](#).



943 **11. Author Contribution**

944 GDV and JPE designed the models and the simulations. FJ, ET, and CT setup the models and
945 conducted the model simulations with contributions from JPE, JK, JA, DC, CR, SW, YL, MER, RG
946 and JL. GDV prepared the manuscript with contributions from all co-authors.

947 **12. Competing Interests**

948 The authors declare that they have no conflict of interest, noting that JK is a Topic Editor of
949 Geoscientific Model Development.

950 **13. Funding**

951 This research was supported by the New South Wales Department of Climate Change, Energy, the
952 Environment and Water as part of the NARClIM2.0 dynamical downscaling project contributing to
953 CORDEX Australasia. Funding was provided by the NSW Climate Change Fund for NSW and
954 Australia Regional Climate Modelling (NARClIM) Project. This research was undertaken with the
955 assistance of resources and services from the National Computational Infrastructure (NCI), which is
956 supported by the Australian Government.

957 **14. References**

- 958 Andrys, J., Lyons, T. J., and Kala, J.: Evaluation of a WRF ensemble using GCM boundary conditions
959 to quantify mean and extreme climate for the southwest of Western Australia (1970–1999),
960 International Journal of Climatology, 36, 4406–4424, <https://doi.org/10.1002/joc.4641>, 2016.
- 961 Australian Bureau of Statistics.: Regional population, Online at:
962 <https://www.abs.gov.au/statistics/people/population/regional-population/latest-release>, 2024.
- 963 Bishop, C. H. and Abramowitz, G.: Climate model dependence and the replicate Earth paradigm,
964 Clim. Dyn., 41, 885–900, 10.1007/s00382-012-1610-y, 2013.
- 965 Bjordal, J., Storelvmo, T., Alterskjaer, K., and Carlsen, T.: Equilibrium climate sensitivity above 5
966 degrees C plausible due to state-dependent cloud feedback, Nat. Geosci., 13, 718+,
967 10.1038/s41561-020-00649-1, 2020.
- 968 Bureau of Meteorology.: Annual climate statement 2016, 2017.
- 969 Chen, F., Liu, C. H., Dudhia, J., and Chen, M.: A sensitivity study of high-resolution regional climate
970 simulations to three land surface models over the western United States, Journal of
971 Geophysical Research-Atmospheres, 119, 7271–7291, 10.1002/2014jd021827, 2014a.
- 972 Chen, F., Barlage, M., Tewari, M., Rasmussen, R., Jin, J. M., Lettenmaier, D., Livneh, B., Lin, C. Y.,
973 Miguez-Macho, G., Niu, G. Y., Wen, L. J., and Yang, Z. L.: Modeling seasonal snowpack



- 974 evolution in the complex terrain and forested Colorado Headwaters region: A model
975 intercomparison study, *Journal of Geophysical Research-Atmospheres*, 119, 13795-13819,
976 10.1002/2014jd022167, 2014b.
- 977 Constantinidou, K., Hadjinicolaou, P., Zittis, G., and Lelieveld, J.: Performance of Land Surface
978 Schemes in the WRF Model for Climate Simulations over the MENA-CORDEX Domain,
979 *Earth Systems and Environment*, 19, 10.1007/s41748-020-00187-1, 2020.
- 980 Dee, D. P., Uppala, S. M., Simmons, A. J., Berrisford, P., Poli, P., Kobayashi, S., Andrae, U.,
981 Balmaseda, M. A., Balsamo, G., Bauer, P., Bechtold, P., Beljaars, A. C. M., van de Berg, L.,
982 Bidlot, J., Bormann, N., Delsol, C., Dragani, R., Fuentes, M., Geer, A. J., Haimberger, L.,
983 Healy, S. B., Hersbach, H., Hólm, E. V., Isaksen, L., Kållberg, P., Köhler, M., Matricardi, M.,
984 McNally, A. P., Monge-Sanz, B. M., Morcrette, J. J., Park, B. K., Peubey, C., de Rosnay, P.,
985 Tavolato, C., Thépaut, J. N., and Vitart, F.: The ERA-Interim reanalysis: configuration and
986 performance of the data assimilation system, *Quarterly Journal of the Royal Meteorological
987 Society*, 137, 553-597, 10.1002/qj.828, 2011.
- 988 Department of Water and Environmental Regulation (DWER): Climate Adaptation Strategy -
989 Building WA's Climate Resilient Future, Government of Western Australia, 25 pages. Online
990 at: https://www.wa.gov.au/system/files/2023-07/climate_adaption_strategy_220623.pdf.
- 991 Di Virgilio, G., Evans, J. P., Di Luca, A., Olson, R., Argüeso, D., Kala, J., Andrys, J., Hoffmann, P.,
992 Katzfey, J. J., and Rockel, B.: Evaluating reanalysis-driven CORDEX regional climate
993 models over Australia: model performance and errors, *Clim. Dyn.*, 53, 2985-3005,
994 10.1007/s00382-019-04672-w, 2019.
- 995 Di Virgilio, G., Ji, F., Tam, E., Nishant, N., Evans, J. P., Thomas, C., Riley, M. L., Beyer, K., Grose,
996 M. R., Narsey, S., and Delage, F.: Selecting CMIP6 GCMs for CORDEX Dynamical
997 Downscaling: Model Performance, Independence, and Climate Change Signals, *Earth's
998 Future*, 10, e2021EF002625, <https://doi.org/10.1029/2021EF002625>, 2022.
- 999 Di Virgilio, G., Ji, F., Tam, E., Evans, J. P., Kala, J., Andrys, J., Thomas, C., Choudhury, D., Rocha,
1000 C., Li, Y., Riley, M.: Evaluation of CORDEX ERA5-forced 'NARClIM2. 0' regional climate
1001 models over Australia using the Weather Research and Forecasting (WRF) model version
1002 4.1.2, *Geoscientific Model Development*, <https://doi.org/10.5194/gmd-2024-41>, In review.
- 1003 Evans, A., Jones, D., Lellyett, S., and Smalley, R.: An Enhanced Gridded Rainfall Analysis Scheme
1004 for Australia, *Australian Bureau of Meteorology*2020a.
- 1005 Evans, J. P., Ji, F., Lee, C., Smith, P., Argüeso, D., and Fita, L.: Design of a regional climate
1006 modelling projection ensemble experiment - NARClIM, *Geosci. Model Dev.*, 7, 621-629,
1007 10.5194/gmd-7-621-2014, 2014.
- 1008 Evans, J. P., Di Virgilio, G., Hirsch, A. L., Hoffmann, P., Remedio, A. R., Ji, F., Rockel, B., and
1009 Coppola, E.: The CORDEX-Australasia ensemble: evaluation and future projections, *Clim.
1010 Dyn.*, 10.1007/s00382-020-05459-0, 2020b.



- 1011 Fiddes, S., Pepler, A., Saunders, K., and Hope, P.: Redefining southern Australia's climatic regions
1012 and seasons, *J. South Hemisph. Earth Syst. Sci.*, 71, 92-109, <https://doi.org/10.1071/ES20003>,
1013 2021.
- 1014 Giorgi, F.: Thirty Years of Regional Climate Modeling: Where Are We and Where Are We Going
1015 next?, *Journal of Geophysical Research: Atmospheres*, 124, 5696-5723,
1016 10.1029/2018jd030094, 2019.
- 1017 Glotfelty, T., Ramírez-Mejía, D., Bowden, J., Ghilardi, A., and West, J. J.: Limitations of WRF land
1018 surface models for simulating land use and land cover change in Sub-Saharan Africa and
1019 development of an improved model (CLM-AF v. 1.0), *Geosci. Model Dev.*, 14, 3215-3249,
1020 10.5194/gmd-14-3215-2021, 2021.
- 1021 Grose, M., Narsey, S., Trancoso, R., Mackallah, C., Delage, F., Dowdy, A., Di Virgilio, G.,
1022 Watterson, I., Dobrohotoff, P., Rashid, H. A., Rauniyar, S., Henley, B., Thatcher, M., Syktus,
1023 J., Abramowitz, G., Evans, J. P., Su, C.-H., and Takbash, A.: A CMIP6-based multi-model
1024 downscaling ensemble to underpin climate change services in Australia, *Climate Services*, 30,
1025 100368, <https://doi.org/10.1016/j.cliser.2023.100368>, 2023.
- 1026 Grose, M. R., Foster, S., Risbey, J. S., Osbrough, S., and Wilson, L.: Using indices of atmospheric
1027 circulation to refine southern Australian winter rainfall climate projections, *Clim. Dyn.*,
1028 10.1007/s00382-019-04880-4, 2019.
- 1029 Grose, M. R., Narsey, S., Delage, F., Dowdy, A. J., Bador, M., Boschat, G., Chung, C., Kajtar, J.,
1030 Rauniyar, S., Freund, M., Lyu, K., Rashid, H. A., Zhang, X., Wales, S., Trenham, C.,
1031 Holbrook, N. J., Cowan, T., Alexander, L. V., Arblaster, J. M., and Power, S. B.: Insights
1032 from CMIP6 for Australia's future climate, *Earth's Future*, 8, e2019EF001469,
1033 <https://doi.org/10.1029/2019EF001469>, 2020.
- 1034 Herger, N., Abramowitz, G., Knutti, R., Angéllil, O., Lehmann, K., and Sanderson, B. M.: Selecting a
1035 climate model subset to optimise key ensemble properties, *Earth Syst. Dynam.*, 9, 135-151,
1036 10.5194/esd-9-135-2018, 2018.
- 1037 Hong, S.-Y., Noh, Y., and Dudhia, J.: A New Vertical Diffusion Package with an Explicit Treatment
1038 of Entrainment Processes, *Monthly Weather Review*, 134, 2318-2341,
1039 <https://doi.org/10.1175/MWR3199.1>, 2006.
- 1040 Hsiang, S., Kopp, R., Jina, A., Rising, J., Delgado, M., Mohan, S., Rasmussen, D. J., Muir-Wood, R.,
1041 Wilson, P., Oppenheimer, M., Larsen, K., and Houser, T.: Estimating economic damage from
1042 climate change in the United States, *Science*, 356, 1362-1368, 10.1126/science.aal4369, 2017.
- 1043 Huang, Y., Xue, M., Hu, X.-M., Martin, E., Novoa, H. M., McPherson, R. A., Perez, A., and Morales,
1044 I. Y.: Convection-Permitting Simulations of Precipitation over the Peruvian Central Andes:
1045 Strong Sensitivity to Planetary Boundary Layer Parameterization, *J. Hydrometeorol.*, 24,
1046 1969-1990, <https://doi.org/10.1175/JHM-D-22-0173.1>, 2023.



- 1047 Imran, H. M., Kala, J., Ng, A. W. M., and Muthukumar, S.: An evaluation of the performance of a
1048 WRF multi-physics ensemble for heatwave events over the city of Melbourne in southeast
1049 Australia, *Clim. Dyn.*, 50, 2553-2586, 10.1007/s00382-017-3758-y, 2018.
- 1050 IPCC: Climate Change 2021: The Physical Science Basis. Contribution of Working Group I to the
1051 Sixth Assessment Report of the Intergovernmental Panel on Climate Change, Cambridge
1052 University Press, 2021.
- 1053 Iturbide, M., Gutiérrez, J. M., Alves, L. M., Bedia, J., Cerezo-Mota, R., Gimadevilla, E., Cofiño, A.
1054 S., Di Luca, A., Faria, S. H., Gorodetskaya, I. V., Hauser, M., Herrera, S., Hennessy, K.,
1055 Hewitt, H. T., Jones, R. G., Krakovska, S., Manzanar, R., Martínez-Castro, D., Narisma, G.
1056 T., Nurhati, I. S., Pinto, I., Seneviratne, S. I., van den Hurk, B., and Vera, C. S.: An update of
1057 IPCC climate reference regions for subcontinental analysis of climate model data: definition
1058 and aggregated datasets, *Earth Syst. Sci. Data*, 12, 2959-2970, 10.5194/essd-12-2959-2020,
1059 2020.
- 1060 Kendon, E. J., Prein, A. F., Senior, C. A., and Stirling, A.: Challenges and outlook for convection-
1061 permitting climate modelling, *Philosophical transactions. Series A, Mathematical, physical,
1062 and engineering sciences*, 379, 20190547, 10.1098/rsta.2019.0547, 2021.
- 1063 Kusaka, H. and Kimura, F.: Coupling a Single-Layer Urban Canopy Model with a Simple
1064 Atmospheric Model: Impact on Urban Heat Island Simulation for an Idealized Case, *Journal
1065 of the Meteorological Society of Japan. Ser. II*, 82, 67-80, 10.2151/jmsj.82.67, 2004.
- 1066 Lee, D., Min, S.-K., Ahn, J.-B., Cha, D.-H., Shin, S.-W., Chang, E.-C., Suh, M.-S., Byun, Y.-H., and
1067 Kim, J.-U.: Uncertainty analysis of future summer monsoon duration and area over East Asia
1068 using a multi-GCM/multi-RCM ensemble, *Environ. Res. Lett.*, 18, 064026, 10.1088/1748-
1069 9326/acd208, 2023.
- 1070 Lucas-Picher, P., Argüeso, D., Brisson, E., Trambly, Y., Berg, P., Lemonsu, A., Kotlarski, S., and
1071 Caillaud, C.: Convection-permitting modeling with regional climate models: Latest
1072 developments and next steps, *WIREs Climate Change*, 12, e731,
1073 <https://doi.org/10.1002/wcc.731>, 2021.
- 1074 Meehl, G. A., Senior, C. A., Eyring, V., Flato, G., Lamarque, J.-F., Stouffer, R. J., Taylor, K. E., and
1075 Schlund, M.: Context for interpreting equilibrium climate sensitivity and transient climate
1076 response from the CMIP6 Earth system models, *Science Advances*, 6, eaba1981,
1077 10.1126/sciadv.aba1981, 2020.
- 1078 Murphy, B. F. and Timbal, B.: A review of recent climate variability and climate change in
1079 southeastern Australia, *International Journal of Climatology*, 28, 859-879,
1080 <https://doi.org/10.1002/joc.1627>, 2008.
- 1081 New South Wales Government.: NSW Climate Change Fund Annual Report 2021-22, 2022.
- 1082 New South Wales Government.: NSW Climate Change Fund Annual Report 2022-23, 2023.



- 1083 Nishant, N., Evans, J. P., Di Virgilio, G., Downes, S. M., Ji, F., Cheung, K. K. W., Tam, E., Miller, J.,
1084 Beyer, K., and Riley, M. L.: Introducing NARcliM1.5: Evaluating the Performance of
1085 Regional Climate Projections for Southeast Australia for 1950–2100, *Earth's Future*, 9,
1086 e2020EF001833, <https://doi.org/10.1029/2020EF001833>, 2021.
- 1087 Niu, G.-Y., Yang, Z.-L., Mitchell, K. E., Chen, F., Ek, M. B., Barlage, M., Kumar, A., Manning, K.,
1088 Niyogi, D., Rosero, E., Tewari, M., and Xia, Y.: The community Noah land surface model
1089 with multiparameterization options (Noah-MP): 1. Model description and evaluation with
1090 local-scale measurements, *Journal of Geophysical Research: Atmospheres*, 116,
1091 10.1029/2010jd015139, 2011.
- 1092 Nuryanto, D. E., Satyaningsih, R., Nuraini, T. A., Rizal, J., Heriyanto, E., Linarka, U. A., and
1093 Sopaheluwakan, A.: Evaluation of Planetary Boundary Layer (PBL) schemes in simulating
1094 heavy rainfall events over Central Java using high resolution WRF model, Sixth International
1095 Symposium on LAPAN-IPB Satellite, SPIE2019.
- 1096 Pepler, A. and Dowdy, A.: Intense east coast lows and associated rainfall in eastern Australia, *J. South
1097 Hemisph. Earth Syst. Sci.*, 71, 110-122, 10.1071/es20013, 2021.
- 1098 Perkins, S. E., Pitman, A. J., Holbrook, N. J., and McAneney, J.: Evaluation of the AR4 climate
1099 models' simulated daily maximum temperature, minimum temperature, and precipitation over
1100 Australia using probability density functions, *J. Clim.*, 20, 4356-4376, 10.1175/jcli4253.1,
1101 2007.
- 1102 Salamanca, F., Zhang, Y. Z., Barlage, M., Chen, F., Mahalov, A., and Miao, S. G.: Evaluation of the
1103 WRF-Urban Modeling System Coupled to Noah and Noah-MP Land Surface Models Over a
1104 Semiarid Urban Environment, *Journal of Geophysical Research-Atmospheres*, 123, 2387-
1105 2408, 10.1002/2018jd028377, 2018.
- 1106 Sherwood, S. C., Webb, M. J., Annan, J. D., Armour, K. C., Forster, P. M., Hargreaves, J. C., Hegerl,
1107 G., Klein, S. A., Marvel, K. D., Rohling, E. J., Watanabe, M., Andrews, T., Braconnot, P.,
1108 Bretherton, C. S., Foster, G. L., Hausfather, Z., von der Heydt, A. S., Knutti, R., Mauritsen,
1109 T., Norris, J. R., Proistosescu, C., Rugenstein, M., Schmidt, G. A., Tokarska, K. B., and
1110 Zelinka, M. D.: An Assessment of Earth's Climate Sensitivity Using Multiple Lines of
1111 Evidence, *Rev. Geophys.*, 58, e2019RG000678, <https://doi.org/10.1029/2019RG000678>,
1112 2020.
- 1113 Skamarock, W. C., Klemp, J. B., Dudhia, J., Gill, D. O., Barker, D. M., Wang, W., and Powers, J. G.:
1114 A description of the Advanced Research WRF Version 3. NCAR Tech Note NCAR/TN-
1115 475+STR. NCAR, Boulder, CO, 2008.
- 1116 Tegen, I., Hollrig, P., Chin, M., Fung, I., Jacob, D., and Penner, J.: Contribution of different aerosol
1117 species to the global aerosol extinction optical thickness: Estimates from model results,
1118 *Journal of Geophysical Research: Atmospheres*, 102, 23895-23915,
1119 <https://doi.org/10.1029/97JD01864>, 1997.



- 1120 Torma, C., Giorgi, F., and Coppola, E.: Added value of regional climate modeling over areas
1121 characterized by complex terrain—Precipitation over the Alps, *Journal of Geophysical*
1122 *Research: Atmospheres*, 120, 3957-3972, 10.1002/2014JD022781, 2015.
- 1123 WCRP: CORDEX experiment design for dynamical downscaling of CMIP6 (DRAFT),
1124 [https://cordex.org/wp-content/uploads/2020/06/CORDEX-
CMIP6_exp_design_draft_20200610.pdf](https://cordex.org/wp-content/uploads/2020/06/CORDEX-
1125 CMIP6_exp_design_draft_20200610.pdf), 2020.
- 1126 WCRP: CORDEX-CMIP6 Data Request, Coordinated Regional Downscaling Experiment
1127 (CORDEX), [https://cordex.org/wp-content/uploads/2022/03/CORDEX-
CMIP6_Data_Request_tutorial.pdf](https://cordex.org/wp-content/uploads/2022/03/CORDEX-
1128 CMIP6_Data_Request_tutorial.pdf), 2022.
- 1129 Whetton, P. and Hennessy, K.: Potential benefits of a “storyline” approach to the provision of regional
1130 climate projection information, *International Climate Change Adaptation Conference*,
1131 NCARF, Gold Coast, Australia2010.
- 1132 Zhuo, L., Dai, Q., Han, D., Chen, N., and Zhao, B.: Assessment of simulated soil moisture from WRF
1133 Noah, Noah-MP, and CLM land surface schemes for landslide hazard application, *Hydrol.*
1134 *Earth Syst. Sci.*, 23, 4199-4218, 10.5194/hess-23-4199-2019, 2019.